Lung Cancer 75 (2012) 313–320

Contents lists available at SciVerse ScienceDirect

Lung Cancer

journal homepage: www.elsevier.com/locate/lungcan

Clonality status of multifocal lung adenocarcinomas based on the mutation patterns of *EGFR* and *K-ras*

Kazuya Takamochi[a], Shiaki Oh[a], Joe Matsuoka[b], Kenji Suzuki[a,*]

[a] *Department of General Thoracic Surgery, Juntendo University School of Medicine, 1-3, Hongo 3-chome, Bunkyo-ku, Tokyo 113-8431, Japan*
[b] *Clinical Research Center and The Center for Lifetime Cancer Education, Juntendo University School of Medicine, 1-3, Hongo 3-chome, Bunkyo-ku, Tokyo 113-8431, Japan*

ARTICLE INFO

Article history:
Received 21 May 2011
Received in revised form 10 August 2011
Accepted 13 August 2011

Keywords:
Adenocarcinoma
Multiple primary lung cancer
Pulmonary metastasis
Epidermal growth factor receptor
K-ras
Clonality

ABSTRACT

Purpose: The purpose of this study is to clarify the clonality status of multifocal lung adenocarcinomas based on the mutation patterns of *epidermal growth factor receptor* (*EGFR*) and *K-ras*.
Methods: We analyzed 82 multifocal lung adenocarcinomas from 36 patients who underwent surgical resection. Genomic DNA was extracted from formalin-fixed, paraffin-embedded tissue and analyzed for *EGFR* and *K-ras* mutations. We determined the clonality status of multifocal lung adenocarcinomas based on the mutation patterns of *EGFR* and *K-ras*. The actuarial survival time was estimated and the prognostic factors were evaluated for 31 patients with synchronous multifocal lung adenocarcinomas.
Results: *EGFR* and *K-ras* mutations were detected in 36 (44%) and 19 (23%) of the 82 tumors, respectively. *EGFR* mutations had occurred randomly in 20 (91%) of the 22 patients with at least one *EGFR* mutated tumor. *K-ras* mutations had occurred randomly in 14 (93%) of the 15 patients with at least one *K-ras* mutated tumor. Combining the results for the *EGFR* and *K-ras* mutation patterns, the clonality status of multifocal lung adenocarcinomas could be determined in 30 (83%) of the 36 patients. No statistically significant difference in the actuarial survival of the patient subgroups stratified according to the clonality status, which was based on the presence of *EGFR* and *K-ras* mutations, was observed.
Conclusions: Both *EGFR* and *K-ras* mutations frequently occur randomly in multifocal lung adenocarcinomas. Combined mutation pattern analyses of *EGFR* and *K-ras* may be useful for making decisions regarding treatment strategies for patients with multifocal lung adenocarcinomas.

1. Introduction

Adenocarcinoma is now the most common histological type of lung cancer, followed by squamous cell carcinoma and small cell carcinoma. Bronchioloalveolar carcinoma (BAC) is a specific subtype of adenocarcinoma that disproportionately affects women, Asians, and non-smokers [1]. Adenocarcinomas, including BACs, frequently develop as synchronous and/or metachronous multifocal disease [2]. Although surgical resection is considered to be the best means of obtaining a definitive diagnosis and curative treatment, resecting all the lesions completely is sometimes difficult in patients with a poor cardiopulmonary function or those with numerous pulmonary lesions.

Epidermal growth factor receptor (*EGFR*) mutation is the most important predictor of the efficacy of EGFR tyrosine kinase inhibitors (TKIs) such as gefitinib and erlotinib [3–7]. In contrast, *K-ras* mutations are a useful biomarker of resistance to EGFR-TKIs [5]. Therefore, if multifocal lung adenocarcinomas simultaneously harbor *EGFR* mutations, they can likely be managed successfully using EGFR-TKIs. But, if they simultaneously harbor *K-ras* mutations, the use of EGFR-TKIs is not preferred. If *EGFR* and *K-ras* mutations are random events in multifocal lung adenocarcinomas, the efficacy of EGFR-TKIs would be limited to only the tumors carrying *EGFR* mutations, and not to those carrying *K-ras* mutations.

The purpose of this study was to clarify the clonality status of multifocal lung adenocarcinomas. The present study, to our knowledge, is the largest investigation of the clonality status of multifocal lung adenocarcinomas based on the mutation patterns of *EGFR* and *K-ras*.

2. Materials and methods

This retrospective review was performed under a waiver of authorization approved by the institutional review board of Juntendo University School of Medicine.

2.1. Patients

Between September 1996 and December 2008, 1047 patients with primary lung cancers underwent pulmonary resection. Among

* Corresponding author. Tel.: +81 3 3813 3111; fax: +81 3 5800 0281.
E-mail address: kjsuzuki@juntendo.ac.jp (K. Suzuki).

0169-5002/$ – see front matter © 2011 Elsevier Ireland Ltd. All rights reserved.
doi:10.1016/j.lungcan.2011.08.007

them, 57 patients had synchronous or metachronous multifocal lung cancers. Patients with pneumonic-type mucinous BAC were excluded. Patients whose tumor tissues were not available for molecular analyses were also excluded. Therefore, we conducted a retrospective review of a total of 82 multifocal lung adenocarcinomas in 36 patients.

2.2. Histological examination

The differential diagnosis of multiple primary lung cancer (MPLC) or pulmonary metastasis (PM) was clinicopathologically performed according to the criteria proposed by Martini and Melamed [8]. The proportion of the BAC component was evaluated microscopically on all the slides, including the largest cut surface of the tumor, using hematoxylin and eosin staining and elastica van Gieson staining. The BAC component was defined as the component of lepidic growth patterns of tumor cells.

2.3. Molecular analyses

DNA extraction and mutation analyses for *EGFR* and *K-ras* were conducted at Mitsubishi Chemical Medience Corporation (Tokyo, Japan). Genomic DNA was extracted from formalin-fixed, paraffin-embedded tissue. Serial slices at 5 μm were made from each block for tumor cell dissection. After deparaffinization with xylene, the tissue sections were stained with hematoxylin and eosin, and the target tumor lesions were macroscopically dissected to minimize contamination with normal tissue. The peptide nucleic acid-locked nucleic acid (PNA-LNA) polymerase chain reaction (PCR) clamp method [9] was used for *EGFR* mutation analysis, while the peptide nucleic acid (PNA)-mediated PCR clamping method [10] was used for the *K-ras* mutation analysis.

2.4. Clonality assessment

In synchronous multifocal tumors, the largest tumor was defined as the "primary tumor" and the remaining tumors were defined as "secondary tumors". In metachronous multifocal tumors, the first tumor was defined as the "primary tumor" and the tumors that developed after the surgical resection of the first tumor were defined as "secondary tumors".

First, we separately compared *EGFR* and *K-ras* mutation statuses between each primary and secondary tumor and classified the results as belonging to one of six different patterns of multifocal tumors (Table 1): pattern A, mutation in only the primary tumor; pattern B, different mutations in the primary and secondary tumors; pattern C, mutation in only the secondary tumor; pattern D, identical mutations in the primary and secondary tumors; pattern E, no mutations both in the primary and secondary tumors; and pattern F, undetermined mutation status in either the primary or secondary tumor regardless of the mutation status in the other tumor. Patterns A, B and C were regarded as indicating different clonal origins, whereas pattern D was regarded as indicating the same clonal origin. Patterns E and F were regarded as indicating an undetermined clonality status.

Table 1
Patterns of *EGFR* and *K-ras* mutations.

Clonality status	Pattern	Primary tumor	Secondary tumor
Different clonality	A	●	○
	B	●	■
	C	○	●
Same clonality	D	●	●
Not determined	E	○	○
	F	Any/?	?/any

EGFR, epidermal growth factor receptor; ●/■, mutation positive; ○, mutation negative; ?, clonality status could not be determined.

Next, we determined the clonality status based on combining the results of the mutation patterns for *EGFR* and *K-ras* genes. A secondary tumor was classified as exhibiting a different clonality if either *EGFR* or *K-ras* mutation belonged to pattern A, B or C but both *EGFR* and *K-ras* mutations did not belong to pattern D. A secondary tumor was classified as exhibiting the same clonality whenever either the *EGFR* or *K-ras* mutation belonged to pattern D. The clonality status was regarded as undetermined for secondary tumors in which both *EGFR* and *K-ras* mutations belonged to either pattern E or F.

2.5. Statistical analysis

The relationships between *EGFR*/*K-ras* mutation status and the clinicopathological features were statistically evaluated using a chi-square test or a Fisher's exact test.

Survival analyses were performed only for the patients with synchronous multifocal adenocarcinomas, since most of the patients (31/36) had synchronous tumors. The length of survival was defined as the interval in days between the day of surgical intervention and the date of either death or the last follow-up. The survival rates were calculated using the Kaplan–Meier method, and the curve differences were tested using the log-rank test. Multivariate analyses of independent prognostic factors were performed using Cox's proportional hazards model. A *P*-value of less than 0.05 was considered statistically significant. All statistical analyses were performed using the SPSS statistical software package (version 17.0, SPSS Inc., Chicago, IL).

3. Results

3.1. Clinicopathological characteristics of patients (Table 2)

The patients comprised 18 men and 18 women. The median age at the time of the first operation was 67 years (range 44–79 years). Twenty-two patients (61%) had a smoking history (either current or ex-smoker). Synchronous multifocal adenocarcinomas were noted in 31 patients (86%) and metachronous ones were noted in 5 patients (16%). The median size of the tumors was 16 mm (range 1–105 mm). Twenty secondary tumors (43%) were located in the same lobe as the primary tumor, and 26 (57%) were located in a different lobe. The number of patients according to the pathological nodal status was 29 with N0, 3 with N1, and 4 with N2, respectively. Therefore, the majority of patients in the present study did not have lymph node involvement.

3.2. Clonality assessment based on EGFR mutation status (Table 2)

EGFR mutations were detected in 36 (44%) of the 82 tumors in total: 20 (56%) of the 36 primary tumors, and 16 (35%) of the 46 secondary tumors. The point mutation L858R in exon 21 and a deletion in exon 19 were detected in 18 and 17 tumors, respectively. T790M in exon 20, which has been recognized as a mutation that confers resistance to EGFR-TKIs, was detected in one tumor.

Simultaneously, two tumors in one patient (No. 16) harbored double *EGFR* mutations and one tumor in one patient (No. 27) had three different types of *EGFR* mutations.

Patient No. 27 had a primary tumor with three different types of *EGFR* mutations and three secondary tumors with one *EGFR* mutation (L858R in exon 21) identical to one in the primary tumor. We classified this patient as having tumors exhibiting the same clonality (pattern D), which corresponds to PM according to the *EGFR* mutation status. Because lung adenocarcinoma is morphologically

Table 2
Clinicopathological characteristics and molecular findings of 82 multifocal lung adenocarcinomas from 36 patients.

Case	P/S	Sex	Age	Pack-year	CEA	M/S	Location of secondary tumors[a]	Tumor size	BAC (%)[b]	pN	PM or MPLC[c]	*EGFR* mutation	*EGFR* mutation pattern	*K-ras* mutation	*K-ras* mutation pattern	Clonality[d]
1	P	F	57	0	4.3	S		32	30	0	MPLC	Ex21: L858R				Same
	S						Same	32	80			Ex21: L858R	D	codon12 AGT	C	
2	P	F	67	0	1.4	S		10	100	0	MPLC			codon12 GCT		Different
	S						Same	2	100				F		A	
3	P	F	44	24	2	S		18	0	0	MPLC					ND
	S						Same	2	70				F		E	
4	P	M	75	55	10.3	S		32	30	0	MPLC	Ex19: L747-T751del				Different
	S						Same	6	60				A		E	
5	P	M	61	10	2.7	S		45	20	2	MPLC			codon12 GAT		Different
	S						Same	5	40				E		A	
6	P	F	78	0	2.9	S		25	40	0	MPLC	Ex19: E746-A750del				Different
	S						Same	1	100				A		E	
7	P	F	68	0	4.3	S		33	40	0	MPLC	Ex21: L858R				Same
	S						Different	16	60			Ex21: L858R	D		E	
8	P	F	60	0.2	3.8	S		50	60	1	MPLC	Ex21: L858R				Same/Different
	S1						Different	3	60				A	codon13 AGC	C	
	S2						Same	5	100			Ex21: L858R	D		E	
9	P	M	58	0	1.2	S		23	40	0	MPLC	Ex19: E746-A750del				Different
	S						Different	5	100			Ex19: del[e]	B		E	
10	P	F	66	20	1.8	S		25	60	0	MPLC	Ex19: L747-E749del Ex19: A750P				Same/Different
	S1						Same	10	60			Ex19: L747-E749del Ex19: A750P	D		E	
	S2						Same	13	60			Ex18: G719S	B		E	
11	P	M	68	86	5.2	M		42	0	0	MPLC			codon12 TGT		Different
	S						Different	18	60				E		A	
12	P	F	74	54	14.1	S		52	80	0	MPLC	Ex19: E746-A750del				Different
	S						Same	6	100				A	codon12 GCT	C	
13	P	F	73	0	3	S		15	50	0	MPLC	Ex21: L858R				Different/Different
	S1						Same	8	100				A		E	
	S2						Different	6	100				A		E	
14	P	M	63	40	3.2	M		20	0	0	MPLC			codon12 GCT		Different
	S						Different	12	10				E		A	
15	P	F	78	0	6.5	S		40	80	0	MPLC			codon12 GAT		Different
	S						Same	7	80			Ex21: L858R	C		A	

Table 2 (*Continued*)

Case	P/S	Sex	Age	Pack-year	CEA	M/S	Location of secondary tumors[a]	Tumor size	BAC (%)[b]	pN	PM or MPLC[c]	*EGFR* mutation	*EGFR* mutation pattern	*K-ras* mutation	*K-ras* mutation pattern	Clonality[d]
16	P	F	60	0	3.1	S		32	5	2	MPLC	Ex21: L858R Ex19: del[e]				Different
	S						Different	6	30			Ex18: G719S Ex19: del[e]	B		E	
17	P	M	78	32.5	1.2	S		29	10	0	MPLC			codon12 GCT		Different
	S						Same	15	100				E	codon12 GTT	B	
18	P	M	72	52	15.2	S		36	0	2	MPLC			codon12 GCT		Different
	S						Different	13	0				E	codon12 TGT	B	
19	P	M	58	0	1.8	S		27	60	0	MPLC	Ex21: L858R				Different/Different
	S1						Different	8	90			Ex19: E746-A750del	B		E	
	S2						Different	22	10				A	codon13 GAC	C	
20	P	M	70	50	0.5	S		20	100	0	MPLC	Ex21: L858R				Different
	S						Different	5	100			Ex19: del[e]	B		E	
21	P	M	66	45	1.8	S		18	20	2	PM					ND
	S						Same	6	10				F		E	
22	P	M	74	90	23.1	S		35	0	0	PM	Ex19: E746-A750del				Different/Different
	S1						Different	25	0				A		E	
	S2						Different	25	0				A		E	
23	P	M	61	21	6.2	S		25	0	1	PM					Different/ND
	S1						Different	7	0				E		E	
	S2						Same	12	0			Ex19: E746-A750del	C		E	
24	P	M	56	19	7.1	S		105	0	0	PM	Ex18: G719S				Different
	S						Different	22	0				A		E	
25	P	M	79	90	3.6	S		70	80	0	PM					ND
	S						Same	7	100				E		E	
26	P	M	49	60	6	M		27	0	0	MPLC					Different
	S						Different	57	0				E	codon12 GAT	C	
27	P	F	68	0	4.2	M		35	40	0	MPLC	Ex19: L747-S752del Ex19: E746V Ex21: L858R Ex20: T790M				Same/Same/Same
	S1						Different	19	70			Ex21: L858R	D		E	
	S2						Different	12	100			Ex21: L858R	D		E	
	S3						Different	12	100			Ex21: L858R	D		E	
28	P	F	78	0	2.4	S		22	60	0	MPLC	Ex18: G719S				Different
	S						Same	20	90				A		E	
29	P	M	63	60	21.3	M		31	70	0	MPLC					Different
	S						Different	15	0				E	codon12 AGT	C	
30	P	F	63	0	1.4	S		21	70	0	MPLC	Ex19: E746-A750del				Different
	S						Different	15	100				A		E	

31	P	F	71	0	1.2	S		8	70	0	MPLC	Ex21: L858R				Same/Different
	S1						Same	3	100				A			
	S2						Different	4	100			Ex21: L858R	D			
32	P	F	74	20	4.7	S		16	60	0	MPLC	Ex21: L858R				Different
	S						Different	15	80			Ex19: L747-T751del	B			
33	P	M	72	138	1.8	S		16	0	1	MPLC					ND
	S						Same	12	0				E			
34	P	F	48	1.8	1.8	S		30	0	0	MPLC			codon12 GAT		Different
	S						Same	4	100				E			
35	P	M	60	40	1.2	S		16	95	0	MPLC	Ex19: E746-A750del		codon12 TGT		Same/Same
	S1						Different	9	90				A	codon12 TGT	D	
	S2						Different	7	80				A	codon12 TGT	D	
36	P	F	67	0	2	S		17	90	0	MPLC					ND
	S						Different	7	100				E			

P, primary tumor; S, secondary tumor; M, male; F, female; CEA, carcinoembryonic antigen; M/S, metachronous/synchronous; BAC, bronchioloalveolar carcinoma; pN, pathological nodal status; MPLC, multiple primary lung cancer; PM, pulmonary metastasis; *EGFR*, epidermal growth factor receptor; ND, not determined.

[a] Location of secondary tumors in comparison to the primary tumor (the same lobe or a different lobe).

[b] Proportion of the BAC component in a tumor.

[c] Differential diagnosis of MPLC or PM based on Martini and Melamed's criteria.

[d] Clonality status based on the presence of *EGFR* and *K-ras* mutations.

[e] Sequence of deleted region in exon 19 could not be determined.

and genetically heterogenous [11], we considered that a clone with the L858R mutation metastasized to three secondary tumors from a primary tumor with genetic heterogeneity.

Twenty-three (50%) secondary tumors were categorized into pattern A, B or C and were regarded as exhibiting a different clonality. Eight (17%) secondary tumors were regarded as exhibiting the same clonality (pattern D). The remaining 15 (33%) were categorized into either pattern E or F, and their clonality status could therefore not be determined. An independent analysis of the *EGFR* mutation status enabled a clonality assessment of multifocal lung adenocarcinomas in 21(58%) of the 36 patients.

EGFR mutations were detected in at least one tumor in 22 patients, and no *EGFR* mutations were detected in any of the tumors in 14 patients. The *EGFR* mutations had occurred randomly in 20 (91%) of the 22 patients. Concordant activating *EGFR* mutations in all the multifocal tumors were detected in the remaining two patients. Different activating *EGFR* mutations in all the multifocal tumors were detected in six of the 20 patients with tumors exhibiting random *EGFR* mutations. In total, some type of activating *EGFR* mutation was found in all the multifocal tumors in eight (22%) of the 36 patients.

3.3. Clonality assessment based on K-ras mutation status (Table 2)

K-ras mutations were detected in 19 (23%) of the 82 tumors in total, 9 (25%) of the 36 primary tumors and 10 (22%) of the 46 secondary tumors. A point mutation in codon 12 was found in 17 tumors, and a point mutation in codon 13 was detected in two tumors. The coexistence of *EGFR* and *K-ras* mutations was observed in 2 (2%) of the 82 lung adenocarcinomas, each from a different patient.

Fourteen (30%) secondary tumors were categorized into pattern A, B or C and were regarded as exhibiting a different clonality. Two (4%) secondary tumors were regarded as exhibiting the same clonality (pattern D). The remaining 30 (65%) were categorized into either pattern E or F. An independent analysis of the *K-ras* mutation status enabled a clonality assessment of multifocal lung adenocarcinomas in 15(42%) of the 36 patients.

K-ras mutations were detected in at least one tumor in 15 patients, and no *K-ras* mutations were detected in any of the tumors in 21 patients. The *K-ras* mutations had occurred randomly in 14 (93%) of the 15 patients.

3.4. Clonality assessment based on combined EGFR and K-ras mutation status (Table 2)

Combining the results for *EGFR* and *K-ras* mutation patterns, 23 (64%) patients were regarded as having tumors with a different clonality, four (11%) patients were regarded as having tumors with the same clonality, and three patients (Nos. 8, 10, and 31) were regarded as having both a tumor with the same clonality and one with a different clonality. Therefore, the clonality status of multifocal adenocarcinomas was determined in 30 (83%) of the 36 patients.

Based on Martini and Melamed's criteria [8], 31 (86%) of the 36 patients were diagnosed as having MPLC and the remaining five (14%) patients were diagnosed as having PM. The results of the clonality assessment based on the combined *EGFR* and *K-ras* mutation status was consistent with the differential diagnosis of MPLC or PM according to Martini and Melamed's criteria in 21 (70%) of the 30 patients whose tumor clonality status could be determined (Table 3).

Table 3
Comparison of differential diagnosis of MPLC or PM based on Martini and Melamed's criteria and a clonality assessment based on *EGFR* and *K-ras* mutation status.

	MPLC[a]	PM[a]
Tumors with a different clonality[b]	21	2
Tumors with the same clonality[b]	4	0
Tumors with a different/the same clonality[b]	3[c]	0
Not determined	3	3

MPLC, multiple primary lung cancer; PM, pulmonary metastasis.
[a] Differential diagnosis of MPLC or PM based on Martini and Melamed's criteria.
[b] Clonality assessment of multifocal adenocarcinomas based on *EGFR* and *K-ras* mutation status.
[c] Three patients (Nos. 8, 10, and 31) had both a secondary tumor with the same clonality and one with a different clonality.

3.5. Relationships between EGFR/K-ras mutation status and clinicopathological features

The relationships between the *EGFR/K-ras* mutation status and the clinicopathological features, such as gender, age, smoking status, preoperative serum carcinoembryonic antigen (CEA) level, pathological nodal status, tumor size, or the proportion of BAC component, were evaluated. Among them, gender and smoking status were associated with the *EGFR* mutation status. The frequency of *EGFR* mutations was significantly higher among women than among men ($P=0.041$) and among never smokers than among current or former smokers ($P=0.014$).

3.6. Survival analyses

The median follow-up period for the 31 patients with synchronous multifocal adenocarcinomas was 40 months (ranging from 6 to 118 months). The overall 3-year and 5-year survival rates were 82.1% and 77.3%, respectively (Fig. 1A). The actuarial survival was significantly higher in female patients than in male patients and in patients with MPLC diagnosed according to Martini and Melamed's criteria than in those with PM (Fig. 1B).

However, no statistically significant differences in actuarial survival were observed among patient subgroups stratified according to age, smoking status, preoperative serum CEA level, pathological nodal status, tumor size, proportion of BAC component, clonality status based on *EGFR* mutations, or clonality status based on *EGFR* and *K-ras* mutations (Fig. 1C) (Table 4).

In a multivariate analysis, the differential diagnosis of MPLC or PM according to Martini and Melamed's criteria was the only significant prognostic factor ($P=0.001$).

4. Discussion

With the recent advance of molecular biology, a number of investigators have performed clonality assessments of multifocal lung cancers using markers such as *p53* mutation [12–15], *K-ras* mutation [16–18], *EGFR* mutation [14,17,18], X-chromosome inactivation [2,13], or loss of heterozygosity analyses of various microsatellite markers [13]. We considered both *EGFR* and *K-ras* to be suitable for investigating the clonal origin of lung adenocarcinomas for the following reasons. First, both *EGFR* [19,20] and *K-ras* mutations [19–21] have been found in atypical adenomatous hyperplasia (AAH), which is considered to be a precursor to lung adenocarcinoma. Moreover, a close relationship between *EGFR* or *K-ras* mutation and lung adenocarcinoma pathogenesis has been demonstrated in transgenic mice [22–24]. Therefore, both *EGFR* and *K-ras* mutations are thought to be early events in lung adenocarcinoma pathogenesis. Second, both *EGFR* and *K-ras* mutations are known to be frequent genetic alterations in lung adenocarcinoma, and these mutations are observed in a mutually exclusive

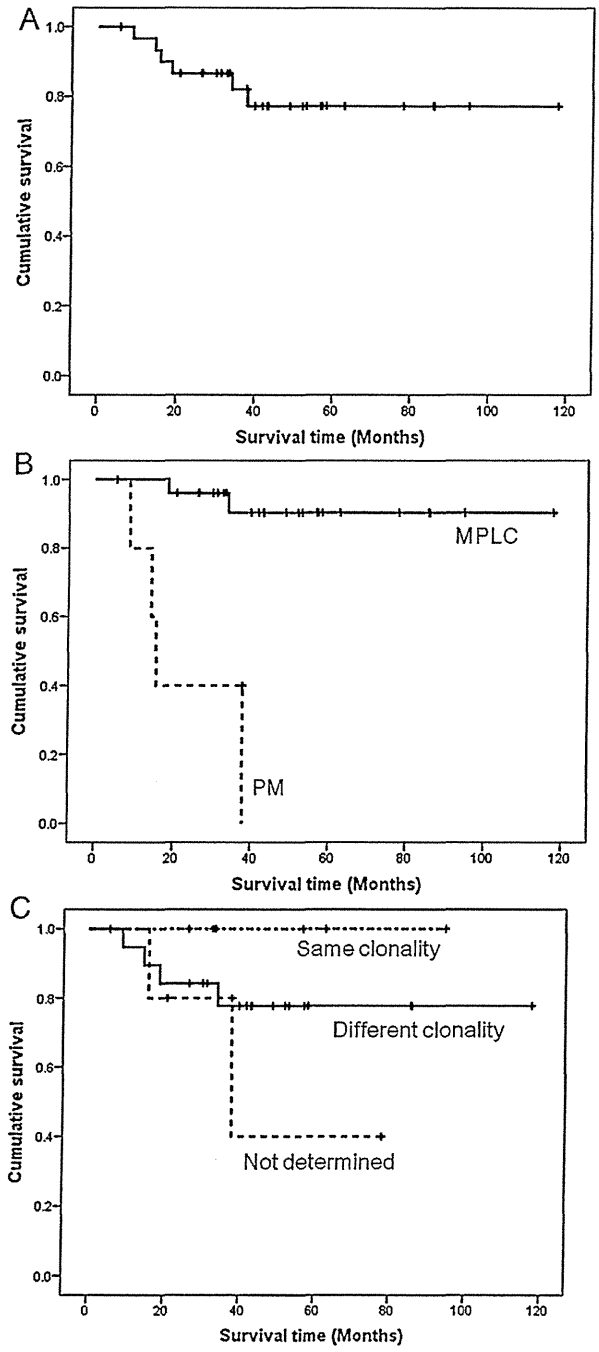

Fig. 1. Survival curves for patients with synchronous multifocal lung adenocarcinomas. (A) Overall patients. (B) Comparison between the outcomes of patients with MPLC and patients with PM diagnosed according to Martini and Melamed's criteria (log-rank test, $P<0.001$). (C) Comparison between the outcomes of patients with tumors exhibiting the same clonality and patients with tumors exhibiting a different clonality based on the presence of *EGFR* and *K-ras* mutations (log-rank test, $P=0.267$).

manner [25]. Therefore, a large portion of multifocal lung adenocarcinomas could be assessed for the clonality status using a combined mutation pattern analysis of *EGFR* and *K-ras*. In the present study, the independent analysis of *EGFR* or *K-ras* mutation status enabled a clonality assessment of multifocal lung adenocarcinomas in 21 (58%) and 15 (42%) of the 36 patients, respectively. However, a clonality assessment was possible in 30 (83%) of the 36

Table 4
Univariate survival analysis of synchronous multifocal lung adenocarcinomas.

Prognostic factors	No.	Survival rates (%)		*P* value[a]
		3-Year	5-Year	
Total	31	82.1	77.3	
Age (years)				
≤65	12	80.2	80.2	0.746
>65	19	83.3	75.8	
Gender				
Male	14	68.4	58.6	0.038
Female	17	94.1	94.1	
Smoking status				
Smoker	18	74.9	66.5	0.158
Nonsmoker	13	92.3	92.3	
Serum CEA level				
Normal	18	79.4	79.4	0.736
Elevated	13	84.6	74.0	
Pathological nodal status				
N0	24	87.5	81.3	0.447
N1 or N2	7	66.7	66.7	
Tumor size				
<30 mm	18	88.2	88.2	0.245
≥30 mm	13	75.2	65.8	
Proportion of BAC component				
<50%	16	65.2	65.2	0.068
≥50%	15	90.0	90.0	
Martini and Melamed's criteria				
MPLC	26	90.4	90.4	<0.001
PM	5	40.0	0.00	
EGFR clonality status				
Same	5	100	100	0.317
Different	16	81.3	81.3	
ND	10	74.1	59.3	
EGFR and *K-ras* clonality status				
Same	6	100	100	0.267
Different	19	77.7	77.7	
vND	6	80.0	40.0	

CEA, carcinoembryonic antigen; BAC, bronchioloalveolar carcinoma; MPLC, multiple primary lung cancer; PM, pulmonary metastasis; *EGFR*, epidermal growth factor receptor; ND: not determined.
[a] Log-rank test.

patients when the results of *EGFR* and *K-ras* mutation analyses were combined.

We showed that both *EGFR* and *K-ras* mutations frequently occurred randomly. Although the numbers of cases were small, several investigators have also reported that *EGFR* and *K-ras* mutations occurred randomly in the same patients with multifocal lung cancers and/or AAHs [18,20,21,26,27]. Multiple primary lung cancers are potentially curable by surgical resection, especially in patients without nodal involvement [28,29]. In this series, no statistical differences in survival were observed between the patients with synchronous multifocal adenocarcinomas exhibiting the same clonality and patients with those exhibiting a different clonality. Therefore, whenever possible, all multifocal adenocarcinomas should be resected in operable patients, regardless of the clonality status.

Recently, in two randomized phase 3 trials, first-line gefitinib monotherapy was shown to improve progression-free survival, compared with standard chemotherapy, in patients with advanced non-small-cell lung cancer harboring *EGFR* mutations [6,7]. EGFR-TKIs could be useful as an alternative treatment for inoperable patients with multifocal adenocarcinomas with activating *EGFR* mutations. In the present series, some type of activating *EGFR* mutation was found in all the multifocal tumors in eight (22%) of the 36 patients. If a surrogate marker for *EGFR* mutations becomes available in the future, these patients may be managed successfully using EGFR-TKIs, since the sampling of all tumors is often impossible practically.

The results of the *EGFR*/*K-ras* clonality assessment were not completely consistent with the differential diagnosis of MPLC or PM according to Martini and Melamed's criteria. In general, differences in genetic alteration patterns are considered to be a good marker for determining tumors of the same (PM) or different origin (MPLC). As shown in the present study, the prognosis of patients with PM according to Martini and Melamed's criteria was worse than that of those with MPLC. However, surprisingly, the clonality status based on *EGFR* and *K-ras* mutations was not prognostic. Although no significant difference was observed, the prognosis of the patients with tumors showing the same clonality was somewhat better than that of those showing a different clonality. All but one patient with synchronous multifocal adenocarcinomas exhibiting the same clonality had *EGFR*-mutated tumors. Therefore, the same *EGFR* mutation might occur simultaneously in a subgroup of multifocal adenocarcinomas through some mechanism other than metastasis. One possibility is the "field effect phenomenon" proposed by Tang et al. [30]. They reported that *EGFR* mutations identical to the tumors were detected in the normal respiratory epithelium in 9 of 21 (43%) patients with *EGFR*-mutated adenocarcinomas but none in patients without mutation in the tumors. A widespread field effect phenomenon caused by some mutagen other than tobacco carcinogen may affect the pathogenesis of multifocal lung adenocarcinoma. Further studies to identify mutagens of *EGFR* are needed to confirm the involvement of the field effect phenomenon in the development of multifocal lung adenocarcinoma.

In summary, *EGFR* and *K-ras* mutations frequently occur randomly in multifocal lung adenocarcinomas. Combined mutation pattern analyses of *EGFR* and *K-ras* may be useful for making decisions regarding treatment strategies for patients with multifocal lung adenocarcinomas. Further well-designed prospective studies with larger numbers of patients are needed to establish guidelines for selecting treatment options, such as surgery or the use of EGFR-TKIs or chemotherapy, based on the *EGFR* and *K-ras* mutation status for patients with multifocal lung adenocarcinomas.

Conflict of interest statement

None declared.

Acknowledgments

This work was supported in part by Takeda Science Foundation, and Grant-in-Aid for Cancer Research (16-1) from the Ministry of Health, Labor and Welfare of Japan.

References

[1] Barsky SH, Cameron R, Osann KE, Tomita D, Holmes EC. Rising incidence of bronchioloalveolar lung carcinoma and its unique clinicopathologic features. Cancer 1994;73:1163–70.
[2] Barsky SH, Grossman DA, Ho J, Holmes EC. The multifocality of bronchioloalveolar lung carcinoma: evidence and implications of a multiclonal origin. Mod Pathol 1994;7:633–40.
[3] Lynch TJ, Bell DW, Sordella R, Gurubhagavatula S, Okimoto RA, Brannigan BW, et al. Activating mutations in the epidermal growth factor receptor underlying responsiveness of non-small-cell lung cancer to gefitinib. N Engl J Med 2004;350:2129–39.
[4] Paez JG, Janne PA, Lee JC, Tracy S, Greulich H, Gabriel S, et al. EGFR mutations in lung cancer: correlation with clinical response to gefitinib therapy. Science 2004;304:1497–500.
[5] Eberhard DA, Johnson BE, Amler LC, Goddard AD, Heldens SL, Herbst RS, et al. Mutations in the epidermal growth factor receptor and in KRAS are predictive and prognostic indicators in patients with non-small-cell lung cancer treated with chemotherapy alone and in combination with erlotinib. J Clin Oncol 2005;23:5900–9.
[6] Maemondo M, Inoue A, Kobayashi K, Sugawara S, Oizumi S, Isobe H, et al. Gefitinib or chemotherapy for non-small-cell lung cancer with mutated EGFR. N Engl J Med 2010;362:2380–8.
[7] Mitsudomi T, Morita S, Yatabe Y, Negoro S, Okamoto I, Tsurutani J, et al. Gefitinib versus cisplatin plus docetaxel in patients with non-small-cell lung cancer

harbouring mutations of the epidermal growth factor receptor (WJTOG3405): an open label, randomised phase 3 trial. Lancet Oncol 2010;11:121–8.
[8] Martini N, Melamed MR. Multiple primary lung cancers. J Thorac Cardiovasc Surg 1975;70:606–12.
[9] Nagai Y, Miyazawa H, Huqun, Tanaka T, Udagawa K, Kato M, et al. Genetic heterogeneity of the epidermal growth factor receptor in non-small cell lung cancer cell lines revealed by a rapid and sensitive detection system, the peptide nucleic acid-locked nucleic acid PCR clamp. Cancer Res 2005;65: 7276–82.
[10] Thiede C, Bayerdorffer E, Blasczyk R, Wittig B, Neubauer A. Simple and sensitive detection of mutations in the ras proto-oncogenes using PNA-mediated PCR clamping. Nucleic Acids Res 1996;24:983–4.
[11] Yoshikawal T, Aoyagi Y, Kodama K, Kamijo T, Yonou H, Yokose T, et al. Topographical distribution of allelic loss in individual lung adenocarcinomas with lymph node metastases. Mod Pathol 2004;17:204–13.
[12] Mitsudomi T, Yatabe Y, Koshikawa T, Hatooka S, Shinoda M, Suyama M, et al. Mutations of the P53 tumor suppressor gene as clonal marker for multiple primary lung cancers. J Thorac Cardiovasc Surg 1997;114:354–60.
[13] Wang X, Wang M, MacLennan GT, Abdul-Karim FW, Eble JN, Jones TD, et al. Evidence for common clonal origin of multifocal lung cancers. J Natl Cancer Inst 2009;101:560–70.
[14] Chang YL, Wu CT, Lin SC, Hsiao CF, Jou YS, Lee YC. Clonality and prognostic implications of p53 and epidermal growth factor receptor somatic aberrations in multiple primary lung cancers. Clin Cancer Res 2007;13:52–8.
[15] van Rens MT, Eijken EJ, Elbers JR, Lammers JW, Tilanus MG, Slootweg PJ. p53 mutation analysis for definite diagnosis of multiple primary lung carcinoma. Cancer 2002;94:188–96.
[16] Holst VA, Finkelstein S, Yousem SA. Bronchioloalveolar adenocarcinoma of lung: monoclonal origin for multifocal disease. Am J Surg Pathol 1998;22:1343–50.
[17] Girard N, Ostrovnaya I, Lau C, Park B, Ladanyi M, Finley D, et al. Genomic and mutational profiling to assess clonal relationships between multiple non-small cell lung cancers. Clin Cancer Res 2009;15:5184–90.
[18] Girard N, Deshpande C, Lau C, Finley D, Rusch V, Pao W, et al. Comprehensive histologic assessment helps to differentiate multiple lung primary nonsmall cell carcinomas from metastases. Am J Surg Pathol 2009;33:1752–64.
[19] Sakamoto H, Shimizu J, Horio Y, Ueda R, Takahashi T, Mitsudomi T, et al. Disproportionate representation of KRAS gene mutation in atypical adenomatous hyperplasia, but even distribution of EGFR gene mutation from preinvasive to invasive adenocarcinomas. J Pathol 2007;212:287–94.
[20] Sartori G, Cavazza A, Bertolini F, Longo L, Marchioni A, Costantini M, et al. A subset of lung adenocarcinomas and atypical adenomatous hyperplasia-associated foci are genotypically related: an EGFR, HER2, and K-ras mutational analysis. Am J Clin Pathol 2008;129:202–10.
[21] Yoshida Y, Shibata T, Kokubu A, Tsuta K, Matsuno Y, Kanai Y, et al. Mutations of the epidermal growth factor receptor gene in atypical adenomatous hyperplasia and bronchioloalveolar carcinoma of the lung. Lung Cancer 2005;50:1–8.
[22] Jackson EL, Willis N, Mercer K, Bronson RT, Crowley D, Montoya R, et al. Analysis of lung tumor initiation and progression using conditional expression of oncogenic K-ras. Genes Dev 2001;15:3243–8.
[23] Ji H, Li D, Chen L, Shimamura T, Kobayashi S, McNamara K, et al. The impact of human EGFR kinase domain mutations on lung tumorigenesis and in vivo sensitivity to EGFR-targeted therapies. Cancer Cell 2006;9:485–95.
[24] Politi K, Zakowski MF, Fan PD, Schonfeld EA, Pao W, Varmus HE. Lung adenocarcinomas induced in mice by mutant EGF receptors found in human lung cancers respond to a tyrosine kinase inhibitor or to down-regulation of the receptors. Genes Dev 2006;20:1496–510.
[25] Shigematsu H, Lin L, Takahashi T, Nomura M, Suzuki M, Wistuba II, et al. Clinical and biological features associated with epidermal growth factor receptor gene mutations in lung cancers. J Natl Cancer Inst 2005;97:339–46.
[26] Chung JH, Choe G, Jheon S, Sung SW, Kim TJ, Lee KW, et al. Epidermal growth factor receptor mutation and pathologic-radiologic correlation between multiple lung nodules with ground-glass opacity differentiates multicentric origin from intrapulmonary spread. J Thorac Oncol 2009;4:1490–5.
[27] Ikeda K, Nomori H, Ohba Y, Shibata H, Mori T, Honda Y, et al. Epidermal growth factor receptor mutations in multicentric lung adenocarcinomas and atypical adenomatous hyperplasias. J Thorac Oncol 2008;3:467–71.
[28] Battafarano RJ, Meyers BF, Guthrie TJ, Cooper JD, Patterson GA. Surgical resection of multifocal non-small cell lung cancer is associated with prolonged survival. Ann Thorac Surg 2002;74:988–93, discussion 93-4.
[29] Pennathur A, Lindeman B, Ferson P, Ninan M, Quershi I, Gooding WE, et al. Surgical resection is justified in non-small cell lung cancer patients with node negative T4 satellite lesions. Ann Thorac Surg 2009;87:893–9.
[30] Tang X, Shigematsu H, Bekele BN, Roth JA, Minna JD, Hong WK, et al. EGFR tyrosine kinase domain mutations are detected in histologically normal respiratory epithelium in lung cancer patients. Cancer Res 2005;65:7568–72.

Human Cancer Biology

Clinical Cancer Research

Upregulation of Notch2 and Six1 Is Associated with Progression of Early-Stage Lung Adenocarcinoma and a More Aggressive Phenotype at Advanced Stages

Takahiro Mimae[1,2], Morihito Okada[1], Man Hagiyama[2,3], Yoshihiro Miyata[1], Yasuhiro Tsutani[1], Takao Inoue[3], Yoshinori Murakami[2], and Akihiko Ito[3]

Abstract

Purpose: Lung adenocarcinoma often manifests as tumors with mainly lepidic growth. The size of invasive foci determines a diagnosis of *in situ*, minimally invasive adenocarcinoma, or invasive types and suggests that some adenocarcinomas undergo malignant progression in that order. This study investigates how transcriptional aberrations in adenocarcinoma cells at the early stage define the clinical phenotypes of adenocarcinoma tumors at the advanced stage.

Experimental Design: We comprehensively searched for differentially expressed genes between preinvasive and invasive cancer cells in one minimally invasive adenocarcinoma using laser capture microdissection and DNA microarrays. We screened expression of candidate genes in 11 minimally invasive adenocarcinomas by reverse transcriptase PCR and examined their involvement in preinvasive-to-invasive progression by transfection studies. We then immunohistochemically investigated the presence of candidate molecules in 64 samples of advanced adenocarcinoma and statistically analyzed the findings, together with clinicopathologic variables.

Results: The transcription factors *Notch2* and *Six1* were upregulated in invasive cancer cells in all 11 minimally invasive adenocarcinomas. Exogenous Notch2 transactivated *Six1* followed by *Smad3*, *Smad4*, and *vimentin*, and enlarged the nuclei of NCI-H441 lung epithelial cells. Immunochemical staining for the transcription factors was double positive in the invasive, but not in the lepidic growth component of a third of advanced Ads, and the disease-free survival rates were lower in such tumors.

Conclusions: Paired upregulation of *Notch2* and *Six1* is a transcriptional aberration that contributes to preinvasive-to-invasive adenocarcinoma progression by inducing epithelial–mesenchymal transition and nuclear atypia. This aberration persisted in a considerable subset of advanced adenocarcinoma and conferred a more malignant phenotype on the subset. *Clin Cancer Res; 18(4); 945–55. ©2011 AACR.*

Introduction

Adenocarcinoma is the most widespread histologic subtype of lung cancer in most countries, accounting for almost half of all lung cancers (1). Lung adenocarcinomas, especially advanced tumors, rarely comprise a single histologic component, and more than 90% of lung adenocarcinomas are of the mixed subtype according to the 2004 WHO classification (2). In an effort to address the complex histologic heterogeneity of adenocarcinomas, a new classification has recently been proposed (3). According to it, a small tumor with the lepidic growth pattern is diagnosed as either adenocarcinoma *in situ* or minimally invasive adenocarcinoma, depending on the presence or absence of microinvasion ($\leq$ 5 mm). If a microinvasion focus of a minimally invasive adenocarcinoma becomes overt (overt invasion; > 5mm), the tumor will be then diagnosed as lepidic-predominant invasive adenocarcinoma. As might be predicted from these diagnostic criteria, to clearly distinguish between adenocarcinoma *in situ* and minimally invasive adenocarcinoma, as well as between minimally invasive adenocarcinoma and lepidic-predominant invasive adenocarcinoma can be difficult. Rather, it seems reasonable to consider that a significant subset of these 3 subtypes is biologically serial and that each subtype represents a different stage of adenocarcinoma progression.

The concept of progression from adenocarcinoma *in situ* to minimally invasive adenocarcinoma is widely accepted (4–9). Noguchi and colleagues noted 2 types of small

Authors' Affiliations: [1]Surgical Oncology, Division of Genome Radiobiology and Medicine, Programs for Biomedical Research, Graduate School of Biomedical Sciences, Hiroshima University, Hiroshima; [2]Division of Molecular Pathology, Institute of Medical Science, University of Tokyo, Tokyo; and [3]Department of Pathology, Faculty of Medicine, Kinki University, Osaka, Japan

Note: Supplementary data for this article are available at Clinical Cancer Research Online (http://clincancerres.aacrjournals.org/).

Corresponding Author: Akihiko Ito, Department of Pathology, Faculty of Medicine, Kinki University, 377-2 Ohno-Higashi, Osaka-Sayama, Osaka 589-8511, Japan. Phone: 81-72-366-0221; Fax: 81-72-360-2028; E-mail: aito@med.kindai.ac.jp

doi: 10.1158/1078-0432.CCR-11-1946

Translational Relevance

Lung adenocarcinomas with mainly lepidic growth component are diagnosed as *in situ*, minimally invasive adenocarcinoma, or lepidic-predominant invasive adenocarcinoma types, depending on the size of invasive foci. In a minimally invasive adenocarcinoma, differentially expressed genes were comprehensively searched between the preinvasive and invasive components, and 2 transcriptional factors, *Notch2* and *Six1*, were identified as genes upregulated in the invasive component in all 11 minimally invasive adenocarcinomas examined. Transfection experiments suggested that Notch2 and Six1 cooperatively induced epithelial–mesenchymal transition of adenocarcinoma cells. Clinicopathologic analyses revealed that upregulation of both Notch2 and Six1 in invasive foci was detected in one-third of 64 lepidic-predominant invasive adenocarcinomas, and these tumors represented an aggressive phenotype. Paired upregulation of *Notch2* and *Six1* seemed to occur during preinvasive-to-invasive adenocarcinoma progression and define a more malignant subset of advanced adenocarcinoma. Notch2 and Six1 are not only useful biomarkers for malignant potential of adenocarcinoma but also can be therapeutic targets in adenocarcinoma.

(maximum diameter, < 2 cm) adenocarcinomas. These are type A (adenocarcinoma *in situ* according to the 2011 classification) that consists entirely of neoplastic cells that grow in lepidic growth pattern and type C (minimally invasive adenocarcinoma according to the 2011 classification) that consists of peripheral lepidic growth and a central microinvasion focus. The 2 types of tumors differ clinicopathologically. (i) After complete resection, patients with type A have 100% disease-specific survival, whereas the 5-year survival rate for patients with type C is 75% (9). (ii) Type C tumors have higher rates of p53 positivity, proliferation, and nuclear atypia than type A (8, 10, 11). Interpreting these data based on the 2011 classification, the microinvasion focus of minimally invasive adenocarcinoma is considered to develop due to the malignant progression of noninvasive, *in situ* neoplastic cells of the lepidic growth component. In contrast to the development of type C or minimally invasive adenocarcinoma tumors, the progression of minimally invasive adenocarcinoma to more advanced forms, including lepidic-predominant invasive adenocarcinoma, has not been studied in detail.

Genetic studies of adenocarcinoma progression have found mutations in *KRAS* and *EGFR* at the preinvasive stage, such as atypical adenomatous hyperplasia and adenocarcinoma *in situ* (12–15), and some adenocarcinomas have the amplification of these genes at the later stage of invasion and metastasis (7, 16, 17). Besides such genomic alterations, specific transcriptional pathways seem to become upregulated during the progression of adenocarcinoma, because recent findings have increasingly clarified that lung cancer progression is promoted by epithelial–mesenchymal transition (EMT; ref. 18) that is controlled by a group of transcription factors that includes Slug, which is a zinc finger type (19). The homeobox transcription factors Oct4 and downstream Nanog both function upstream of Slug to promote EMT in A549 lung adenocarcinoma cells (20). Although lung adenocarcinoma progression is assumed to be a stepwise process triggered by multiple genetic aberrations, which aberration(s) accounts for each process in the stepwise progression requires precise examination.

In this study, we attempted to obtain the genetic evidence, indicating that all or a subset of lepidic-predominant invasive adenocarcinoma develops from minimally invasive adenocarcinoma, and to clarify what clinical phenotypes the subset has. For this purpose, we designed the experiments that were composed of 3 parts. In the first part, we aimed to comprehensively compare the gene expression profiles between lepidic growth and microinvasion cancer cells from a single minimally invasive adenocarcinoma and successfully identified 2 transcription factors *Notch2* and *Six1* as genes upregulated in microinvasion cells. In the second part, we examined whether the identified genes might play causative roles in early-stage adenocarcinoma progression from lepidic growth to microinvasion cells, and found that Notch2 and Six1 coordinately induced EMT and nuclear atypia in lung epithelial cells. Finally in the third part, we immunohistochemically stained 64 specimens of lepidic-predominant invasive adenocarcinoma for Notch2 and Six1 and found that a third were a simple advanced form of minimally invasive adenocarcinoma, judging from the upregulation of Notch2 and Six1 in overt invasion cells. Importantly, the disease-free survival of patients with such tumors was poorer.

Materials and Methods

Sample selection

This study included patients with both consolidated lung tumors and ground glass opacities on chest high-resolution computed tomography images who underwent lobectomy or segmentectomy at Hiroshima University Hospital between 2007 and 2010 (Hiroshima, Japan). All patients provided written, informed consent to participate in this study and our Institutional Review Board approved the protocol (approval number: Hi-29). Half of the cancerous tissues were placed in Ultramount Aqueous Permanent Mounting Medium (DakoCytomation) and frozen for later studies, whereas the other half was preserved in 10% formalin for diagnosis. Gene expression was analyzed in samples of minimally invasive adenocarcinoma from 11 patients and 64 lepidic-predominant invasive adenocarcinoma tumor samples were immunohistochemically stained.

Cell culture

NCI-H441 human lung papillary adenocarcinoma cells, A549 human lung adenocarcinoma cells and MDA-MB-231

human breast cancer cells were purchased from the American Type Culture Collection and RERF-LC-MS human lung adenocarcinoma cells were from Japanese Cancer Research Resources Bank (JCRB, Osaka, Japan) in 2010, and all experimentation using cell lines proceeded within 6 months after resuscitation. NCI-H441 cells and A549 cells were grown in RPMI-1640 (Nacalai Tesque) and Dulbecco's Modified Eagle Medium (Nacalai Tesque) supplemented with 10% FBS, antibiotics containing 100 units/mL penicillin, 100 μg/mL streptomycin (Invitrogen), and 0.01M-HEPES buffer (Nacalai Tesque) at 37°C in 5% CO_2/95% air. RERF-LC-MS cells were grown in Eagle's minimal essential medium (Nacalai Tesque) supplemented with 10% FBS, antibiotics, and 0.1 mmol/L nonessential amino acids (GIBCO-Invitrogen) at 37°C in 5% CO_2/95% air. MDA-MB-231 cells were grown in L-15 (Sigma-Aldrich) medium supplemented with 10% FBS, antibiotics, and 0.3 g/L L-glutamine (Sigma-Aldrich) at 37°C in 100% air.

Laser capture microdissection

Serial 15-μm sections of the 11 frozen minimally invasive adenocarcinoma tumors were stained with hematoxylin. Only cancer cells were selectively and separately collected from the lepidic growth and microinvasion components using laser capture microdissection (LMD7000; Leica Microsystems GmbH). The cancer cells were placed in the caps of collection tubes containing Tris [2-carboxyethyl] phosphine hydrochloride buffer. The collection time for one slide was 30 minutes. Twenty slides were done for each component. Each cell pool was frozen with dry ice immediately after collection.

RNA purification and amplification with Cy3 or Cy5 labeling

Total RNA was extracted from each cell pool using NucleoSpin RNA XS (Macherey-Nagel GmbH & Co. KG) and from one small ($\leq$ 1 cm) minimally invasive adenocarcinoma tumor and then cDNAs and amino allyl aRNA were synthesized from the RNA using Amino Allyl MessageAmp II aRNA Amplification Kits (Applied Biosystems). CyeDye coupling and fragmentation proceeded according to a protocol supplied by Toray Industries Inc. The concentration, purity, and integrity of the amplified and labeled aRNA were determined using a Eukaryotes Total RNA Nano Series II (Agilent Technologies). Total RNA from cultured cells was also extracted using NucleoSpin RNA XS.

Gene microarray analysis

Amplified RNA samples from microinvasion components were analyzed using 3D-Gene Human Oligo chip 25k (Toray Industries Inc.) microarrays of 25,370 distinct genes and RNA samples from lepidic growth components as controls. The 3-dimensional microarrays were constructed with wells as spaces between probes and cylinder stems with 70-mer oligonucleotide probes on the top to promote efficient hybridization. Cy3- or Cy5-labeled aRNA pools in hybridization buffer were hybridized for 16 hours according to the supplier's protocol (www.3d-gene.com). Hybridization signals were scanned using ScanArray Express Scanner (PerkinElmer) and processed using GenePixPro version 5.0 (Molecular Devices). Signals detected for each gene were normalized by global normalization (Cy3/Cy5 ratio median = 1) and Cy3/Cy5 normalized ratios >2.0 or <0.5 were, respectively, defined as commonly upregulated or downregulated genes.

Semiquantitative reverse transcriptase PCR

We analyzed the expression of *Notch2*, *Six1*, *thyroid transcription factor-1* (*TTF-1*), *Smad3*, *Smad4*, *vimentin*, *E-cadherin*, and *GAPDH* mRNA using reverse transcriptase PCR (RT-PCR) using SuperScriptTMIII First-Strand Synthesis SuperMix (Invitrogen) for the RT. In brief, total RNA was incubated with 50 ng of random hexamer primers and 1 μL of annealing buffer at 65°C for 5 minutes. The RNA was then incubated at 25°C for 5 minutes and at 50°C for 50 minutes in a final volume of 20 μL of reaction mixture containing 1× first-strand reaction mix comprising 5 mmol/L $MgCl_2$, 0.5 mmol/L of each deoxynucleotide triphosphate (dNTP), and 2 μL of SuperScriptTMIII/RNaseOUTTM Enzyme Mix.

The cDNA constructs were amplified by PCR using TaKaRa Ex Taq (Takara). The PCR conditions were 35 cycles of 30 seconds at 94°C (denaturation), 30 seconds at 55°C (annealing), and 30 seconds at 72°C (extension). The sense and antisense primers were 5′-AAAAATGGGGCCAACCGAGAC-3′ and 5′-TTCATCCAGAAGGCGCACAA-3′ for human *Notch2*, 5′-ACTCTCTGCTCGGCCCCCTC-3′ and 5′-AAGGCTGCTGAAACAGGCGT-3′ for human *Six1*, 5′-ATGTCGATGAGTCCAAAG-3′ and 5′-TCACCAGGTCCGA-3′ for human *TTF-1*, 5′-CGGGCCATGGAGCTGTGTGA-3′ and 5′-ACCTGCGTCCATGCTGTGGT-3′ for human *Smad3*, 5′-TCAGGGCCTCAGCCAGGACA-3′ and 5′-TCTCCTCCAGAAGGGTCCACGT-3′ for human *Smad4*, 5′-CAAGGGCCAAGGCAAGTCGC-3′ and 5′-GCCGTGAGGTCAGGCTTGGA-3′ for human *vimentin*, 5′-CCCTGGCTTTGACGCCGAGA-3′ and 5′-AAACGGAGGCCTGATGGGGC-3′ for human *E-cadherin*, and 5′-ACCACAGTCCATGCCATCAC-3′ and 5′-TCCACCACCCTGTTGCTGTA-3′ for human *GAPDH*, respectively. The PCR products were resolved by electrophoresis on 1% agarose gels, stained with ethidium bromide, and densitometrically analyzed. The RT-PCR signal intensity was quantified using ImageJ software (NIH) to compare *Notch2*, *Six1*, *TTF-1*, *Smad3*, *Smad4*, *vimentin*, *E-cadherin*, and *GAPDH* mRNA levels.

Construction of plasmid vectors expressing Notch2 intracellular domain, TTF-1, and siRNA against Six1

The cDNA construct for Notch2 intracellular domain (ICD; amino acids 1,703–2,475) inserts was amplified by PCR using KOD FX DNA polymerase (Toyobo Co. Ltd.) with following primer set: sense, 5′-CCGGATCCATGAAGCGTAAG-3′ (containing the first codon of Notch2 ICD); antisense, 5′-CCGTTAACTCACGCATAAACCTG-3′ (containing the stop codon of Notch2 ICD). The *TTF-1* gene produces 2 alternative transcripts, of which the short form consists of more than 90% of the total transcripts (21). The open reading frame of the short form of the cDNA from

NCI-H441 cells was amplified by PCR using the primer set: sense, 5′-CCGAATTCATGTCGATGAGTCCAAAG-3′; antisense, 5′-CCGTTAACTCACCAGGT-CCGA-3′. The PCR products were resolved by electrophoresis on 1% agarose gels and stained with ethidium bromide. Targeted bands were excised from gels and DNA was extracted and purified using the Wizard SV Gel and PCR Clean-Up System (Promega Corporation), as described by the manufacturer. Extracted DNA chains were annealed and ligated into the *Bam*HI/*Hpa*I (for Notch2) and *Eco*RI/*Hpa*I (for TTF-1) sites of pCX4-bsr, a modified pCX-bsr retroviral vector (22) provided by Dr. T. Akagi (Osaka Bioscience Institute, Osaka, Japan), and sequenced.

The pSilencer4.1-CMVneo siRNA plasmid vector (Ambion) was used to construct pSilencer4.1-CMVneo-si-Six1 and the negative control, pSilencer4.1-CMVneo-scramble. A DNA chain with the following sense and antisense sequences was synthesized to target the Six1 sequence: 5′-GATCCCCAGCTCAGAAGAGGAATTTTC-AAGAGAAA-TTCCTCTTCTGAGCTGGTT-3′ (sense) and 5′-AGCTTAACCAGCTCAGAAGAGGAATT-TCTCTTGAA-AATTCCTCTTCTGAGCTGGG-3′ (antisense). The target sequence of the negative control (scramble-pSilencer4.1-CMVneo) was 5′-GATCCCGT-CGATTTTGTGATGCTCG-TCAGTTCAAGAGACTGACGAGCATCACAAAATCGACG-G-TT-3′ (sense) and 5′-AGCTTAACGTCGATTTTGTGA-TGCTCGTCAGTCTCTTGAACTGA-CGAGCATCACAAAAT-CGACGG-3′ (antisense), which has no homology with any human DNA. The DNA chains were annealed and ligated into the *Bam*HI/*Hin*dIII sites of pSilencer4.1-CMVneo to generate pSilencer4.1-CMVneo-si-Six1. The negative control pSilencer4.1-CMVneo-scramble vector was constructed in the same manner. The plasmids were extracted and the accuracy of the constructs was confirmed by sequencing.

Transfection

NCI-H441 cells were transiently transfected with empty pCX4-bsr, pCX4-bsr-Notch2 ICD, or pCX4-bsr-TTF-1 using FuGENE 6 (Roche Applied Science). In brief, 2.0×10^5 cells were seeded on 60-mm culture dishes overnight until 50% to 80% confluence was reached. Serum-free medium (194 μL) and 6.0 μL of FuGENE 6 reagent were mixed in 1.5-mL tubes and incubated for 5 minutes at room temperature. Plasmid vectors (2.0 μg each) were added and the contents were mixed and incubated with transfection reagent and DNA complex for at least 15 minutes at room temperature. The transfection reagent and DNA complex were added drop wise to the cultured cells and incubated for 48 hours. The medium was removed and the cells were rinsed 3 times with PBS. The transfected cells were then used in various experiments. A549, RERF-LC-MS, and MDA-MB-231 were also transiently transfected with empty pCX4-bsr or pCX4-bsr-Notch2 ICD using FuGENE 6.

Double transfection proceeded as follows. NCI-H441 cells were transiently transfected with 2.0 μg of each of pCX4-bsr-Notch2 ICD and the empty pSilencer4.1-CMVneo, or pSilencer4.1-CMVneo-scramble, or pSilencer4.1-CMVneo -si-Six1 using FuGENE 6.

Immunohistochemistry

Tissues fixed with 10% formalin were embedded in paraffin and cut into 4-μm thick sections that were deparaffinized, rehydrated, and autoclaved for 20 minutes at 121°C in 10 mmol/L citrate buffer (pH 6.0) and then incubated in methanol containing 3% peroxide for 5 minutes. The sections were washed 3 times with PBS between all steps of the procedure. Nonspecific Ig binding in the sections was blocked by incubation with PBS containing 2% bovine serum albumin (BSA) for 10 minutes. The sections were then incubated with anti-Notch2 antibody (ab8926, 1:400 dilution; Abcam) and/or anti-Six1 antibody (HPA001893, 1:100 dilution; Sigma-Aldrich) in PBS containing 2% BSA for 2 hours at room temperature, followed by horseradish peroxidase–conjugated anti-rabbit Ig G antibody (1:100 dilution; Santa Cruz) in PBS containing 2% BSA for 2 hours at 4°C. Color was developed using aminoethylcarbazole (DAB; Dako) as the substrate for peroxidase. Tissues were counterstained with hematoxylin and mounted. Negative immunohistochemical control procedures comprised the omission and replacement of primary antibodies with appropriate concentrations of normal rabbit or mouse IgG. Slides were examined using a light microscope (BX51; Olympus) equipped with a CCD camera DP72 (Olympus). The results on the control slides were negative.

Cancer cells were deemed positive for Notch2 when the cytoplasm of over half of the cancer cells in each of the lepidic growth and microinvasion components was intensely stained. Other staining profiles were defined as negative. Cancer cells were deemed positive for Six1 when nuclei in over half of the cancer cells in each of the lepidic growth and microinvasion components were intensely stained. Other staining profiles were defined as negative.

Nuclear size analysis

Five minimally invasive adenocarcinoma tumors that contained a Notch2-negative lepidic growth component and a Notch2-positive microinvasion component were immunohistochemically selected. The greatest nuclear dimension of cancer cells in both the lepidic growth and microinvasion components was separately determined in 5 tumors using hematoxylin and eosin (H&E) staining and light microscopy (BX51). The greatest nuclear dimension of 200 cells was measured in random fields for each component from each tumor. The greatest nuclear dimension of the control and of NCI-H441 cells transfected *in vitro* with empty pCX4-bsr, pCX4-bsr-Notch2 ICD, or pCX4-bsr-TTF-1 was assessed by nuclear staining using 4′,6-diamino-2-phenylindole (DAPI) and the fluorescence microscope, Axio Observer D1 (Carl Zeiss). We determined the nuclear dimensions of 100 cells in randomly selected fields in 3 independent experiments.

Statistical analysis

Data about signal intensity and cell morphology are described as means ± SD or as means ± SE and were analyzed using Student *t* test. The clinicopathologic findings were analyzed using the Mann–Whitney *U* test for

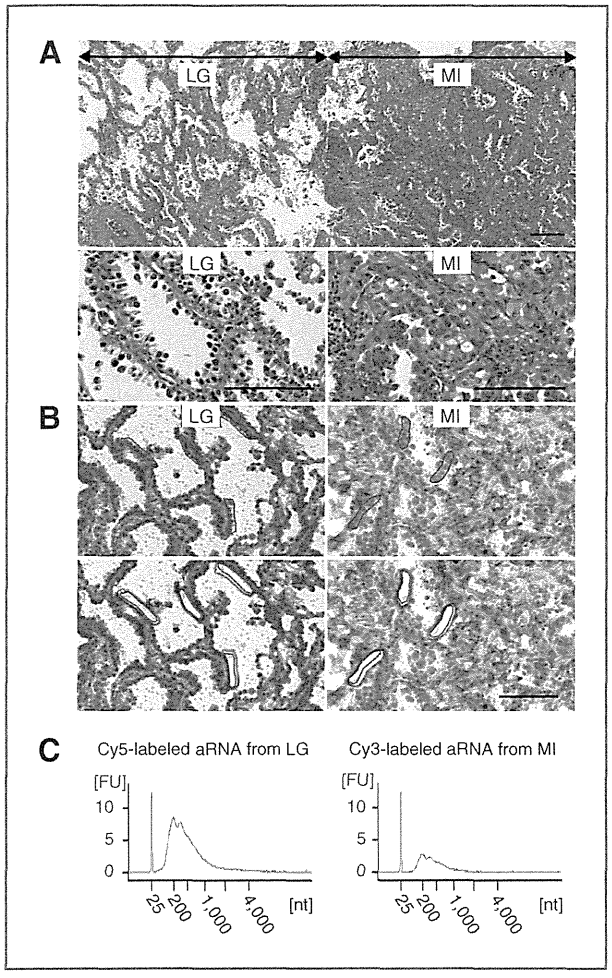

Figure 1. Laser capture microdissection of lepidic growth (LG) and microinvasion (MI) cancer cells from a single minimally invasive adenocarcinoma (case 1) and probe preparation for DNA microarray analysis. A, photomicrograph of minimally invasive adenocarcinoma from case 1 stained with H&E. Top, low-power field view (original magnification, ×100) containing both lepidic growth and microinvasion components; bottom, high-power field view (original magnification, ×400) of each component. B, lepidic growth and microinvasion cancer cells collected by laser capture microdissection from frozen sections of minimally invasive adenocarcinoma tumor. Cancer cells circled in red (top) were cut out using laser pulses run along the circles (bottom). C, verification of aRNA probes for DNA microarray analysis. Total RNA extracted from pools of lepidic growth and microinvasion cancer cells served as templates for preparation of aRNA probes. Quality and quantities of probes were verified by resolving Cy3- or Cy5-labeled aRNA by capillary gel electrophoresis. The amounts of RNA extracted and amplified were 46.2 ng and 14.3 μg for lepidic growth component and 48.4 ng and 4.0 μg for microinvasion component, respectively. Bar, 100 μm.

continuous variables and χ^2 tests for categorical variables. Disease-free survival (DFS) curves were calculated using the Kaplan–Meier method. Univariate and multivariate analyses were done using the log-rank and logistic regression tests, respectively. A P value of ≤ 0.05 was regarded as significant.

Results

Isolation of genes that are differentially expressed in lepidic growth and microinvasion cancer cells in a single minimally invasive adenocarcinoma

A small (1 cm in greatest dimension), solitary lung tumor was surgically resected and histopathologically diagnosed as minimally invasive adenocarcinoma (formerly, type C by Noguchi classification; Fig. 1A; case 1 in Fig. 2A and Supplementary Table S1). We separately isolated lepidic growth and microinvasion cancer cells without contamination from frozen tumor sections using a laser capture microdissection system (Fig. 1B). We extracted total RNAs from about 500 lepidic growth and microinvasion cancer cells and then amplified and labeled the RNAs using T7 RNA polymerase. Fig. 1C shows the amounts and quality of the original total RNAs and amplified aRNAs. The aRNAs were comparatively analyzed using highly sensitive oligo DNA microarrays. The complete gene expression dataset of the microdissected minimally invasive adenocarcinoma specimen is available at Gene Expression Omnibus (GEO) accession number GSE30663 (23). The numbers of genes whose expression levels were double or more and half or less in the microinvasion cancer cells were 2,905 and 2,143, respectively. Supplementary Table S2 shows the top 30 of each of

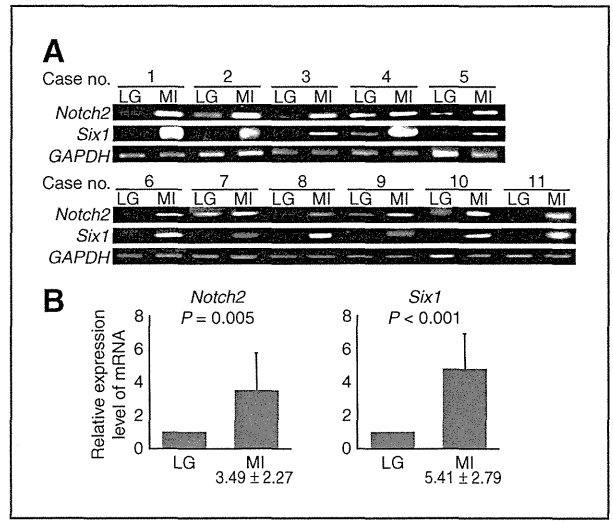

Figure 2. RT-PCR analyses of *Notch2* and *Six1* in total RNA from lepidic growth (LG) and microinvasion (MI) cancer cells in 11 minimally invasive adenocarcinomas. lepidic growth and microinvasion cancer cells were separately collected from frozen sections of minimally invasive adenocarcinomas (cases 1 to 11 listed in Supplementary Table S1) using laser capture microdissection. Total RNAs were extracted from each cell pool and analyzed by RT-PCR using primer sets for *Notch2*, *Six1*, or *GAPDH*. Portions of PCR products were resolved by electrophoresis on 1% agarose gels (A). All band intensities were converted to densitometric values; *Notch2* and *Six1* values were normalized to that of *GAPDH* and then means and SD of 11 minimally invasive adenocarcinomas were calculated. Expression levels of *Notch2* and *Six1* mRNA in microinvasion cancer cells are expressed as relative values normalized to 1 for means in lepidic growth cancer cells (B).

the upregulated (>94-fold) and downregulated (<1/25.4-fold) candidate genes.

Upregulation of Notch2 and its downstream Six1 in microinvasion cancer cells

We found that *Six1* (136-fold) was the most upregulated among the top 30 genes in microinvasion cancer cells, and *Notch2* was 10.7-fold upregulated in the complete dataset. We considered that this paired upregulation was worthy of further investigation because both Six1 and Notch2 can function as transcription factors and Six1 is a putative downstream target of Notch2 (24, 25). As with minimally invasive adenocarcinoma from case 1, we extracted total RNAs from lepidic growth and microinvasion cancer cells separately from minimally invasive adenocarcinomas resected from cases 2 to 11 (Fig. 2A and Supplementary Table S1). *Six1* and *Notch2* mRNA expression was then screened in all 11 minimally invasive adenocarcinomas by semiquantitative RT-PCR. Significantly more mRNA for either gene was found in microinvasion than in lepidic growth cancer cells from all 11 minimally invasive adenocarcinomas (Fig. 2A and B). The expression of Notch2 and Six1 proteins was examined in the case 10 minimally invasive adenocarcinoma by immunohistochemistry. Notch2 and Six1 immunoreactive signals were clearly detected in the cytoplasm and nucleus of microinvasion cancer cells, respectively, whereas lepidic growth component cells were nearly completely negative for the two molecules (Fig. 3).

We speculated whether Notch2 upregulation results in *Six1* transactivation in lung epithelial cells and examined this notion in NCI-H441 cells that have been widely studied as lung epithelial cells. The results of RT-PCR analyses revealed that these cells expressed endogenously undetectable levels of *Notch2* or *Six1* (Fig. 4A, lane 1). Because Notch2 is enzymatically processed to release its ICD that functions as a transcription factor (26), we subcloned Notch2 ICD cDNA into the mammalian expression vector, pCX4-bsr. NCI-H441 cells transfected with this plasmid contained not only abundant exogenous transcripts for Notch2 ICD but also abundant endogenous transcripts for Six1 (Fig. 4A, lane 3 and Supplementary Fig. S1). We also transfected NCI-H441 cells with the cDNA for TTF-1, well known as a lung epithelial transcription factor, but *Six1* transactivation was undetectable (Fig. 4A, lane 4 and Supplementary Fig. S1). Similar experiments using MDA-MB-231 breast cancer cells that express endogenously detectable levels of *Notch2* and *Six1* showed that exogenous Notch2 ICD did not upregulate, but rather slightly downregulated *Six1* (Fig. 4A, lanes 8–10). These results suggested that Notch2 specifically transactivates *Six1* in NCI-H441.

Involvement of Notch2 and Six1 in EMT and nuclear atypism in lung epithelial cells

Notch2 and Six1 promote EMT in various cancers partly through activating the TGF-β intracellular signaling pathways that involve the intracellular signal transducers Smad3 and Smad4 (27–29). Consistent with their epithelioid

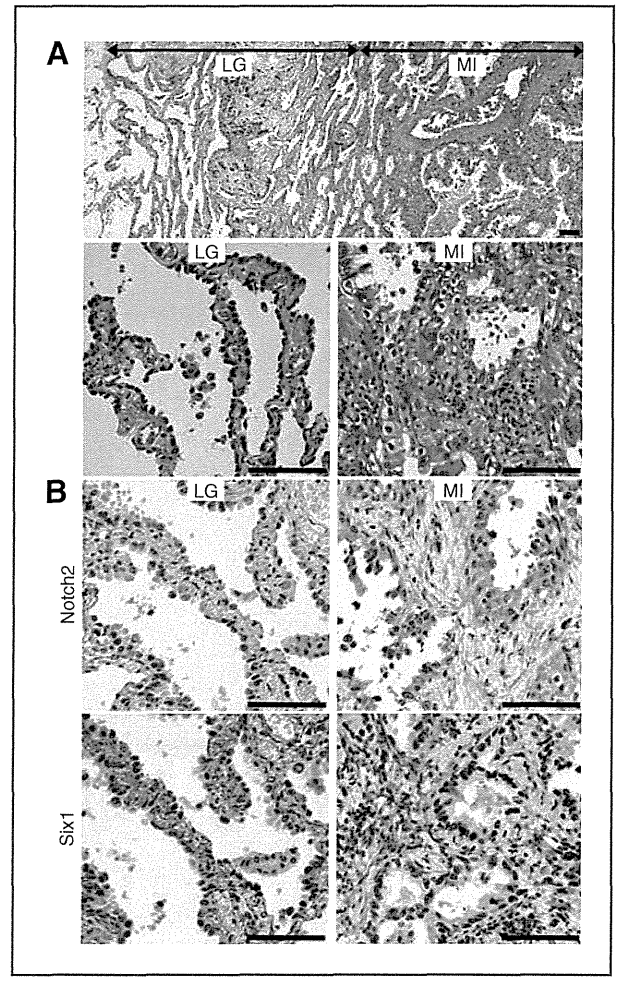

Figure 3. Immunohistochemical staining for Notch2 and Six1 on a minimally invasive adenocarcinoma. Serial sections of the minimally invasive adenocarcinoma from case 10 (listed in Fig. 2A and Supplementary Table S1) were stained with H&E (A) and immunostained with either the Notch2 or Six1 antibody (B). Representative staining images of the lepidic growth (LG) and microinvasion (MI) components are shown in the left and right panels, respectively. Bar, 100 μm.

morphology, NCI-H441 cells expressed easily and faintly detectable levels of *E-cadherin* and *vimentin*, respectively (Fig. 4A, lane 1). The expression levels of these two genes were inverse in NCI-H441 cells transfected with Notch2 ICD cDNA (Fig. 4A, lane 3 and Supplementary Fig. S2). Such transfection also resulted in *Smad3* and *Smad4* transactivation (Fig. 4A, lane 3 and Supplementary Fig. S2). Transfection with the empty vector did not alter the endogenous expression of these 4 genes (Fig. 4A, lane 2 and Supplementary Fig. S2). Transfection with TTF-1 resulted in *vimentin* transactivation and *E-cadherin* downregulation (Fig. 4A, lane 4 and Supplementary Fig. S2). Notch2 seemed to promote EMT in NCI-H441 cells more efficiently than TTF-1. NCI-H441 cells were transfected with Notch2 ICD cDNA and with either Six1-targeting siRNA or a control scrambled siRNA. The Six1-targeting siRNA abrogated not only Notch2 ICD–induced transactivation of *Six1* but also

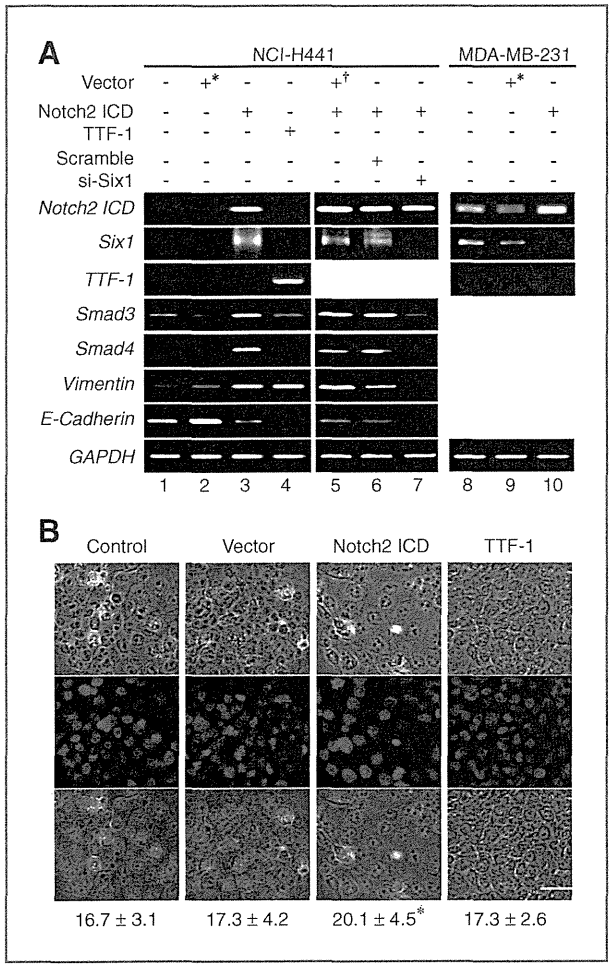

Figure 4. Transcriptional and cell morphologic alterations induced by exogenous Notch2 ICD in NCI-H441 cells. A, expression of EMT-related genes in NCI-H441 and MDA-MB-231 cells before and after transfection with various transcription factors and si-RNA. NCI-H441 and MDA-MB-231 cells were transiently transfected with pCX4-bsr empty (*lanes 2 and 9) or with vectors expressing either Notch2 ICD (lanes 3 and 10) or TTF-1 (lane 4). NCI-H441 cells were transiently transfected in some experiments with Notch2 ICD cDNA and with either empty pSilencer4.1-CMVneo (†lane 5) or vectors expressing scrambled (lane 6) or Six1-targeting (lane 7) siRNA. Total RNAs extracted from intact or transfected cells were analyzed by RT-PCR using primer set for indicated genes. Portions of PCR products were resolved by electrophoresis on 1% agarose gels. B, changes in sizes of nuclei in NCI-H441 cells transfected with Notch2 ICD cDNA. NCI-H441 cells were transfected or not (control) with either empty pCX4-bsr or vectors expressing cDNAs for Notch2 ICD or TTF-1 and then stained with DAPI to visualize nuclei (blue). Phase-contrast (top) and UV laser (middle) images of cells are merged (bottom). Sizes of nuclei were determined as described in Materials and Methods, and calculated means and SE are shown below the images. *, $P < 0.01$ compared with values of other types of cells. Bar, 50 μm.

that of *Smad3*, *Smad4*, and *vimentin*, whereas it further enhanced the Notch2 ICD–induced downregulation of *E-cadherin* (Fig. 4A, lane 7). Control transfection did not alter the gene expression induced by Notch2 ICD (Fig. 4A, lanes 5 and 6). These results indicated that Six1 is essential for Notch2 to transactivate *Smad3*, *Smad4*, and *vimentin*, but not to downregulate *E-cadherin*.

Notch2 ICD transfection experiments, followed by RT-PCR, were conducted on 2 other lung adenocarcinoma cell lines, A549 and RERF-LC-MS, both of which expressed endogenously undetectable levels of Notch2 and Six1 (Supplementary Fig. S3). Exogenous Notch2 ICD in these cells induced gene expression alterations resembling those in NCI-H441 cells, except that *Smad4* and *E-cadherin* were not upregulated in A549 and RERF-LC-MS, respectively (Supplementary Fig. S3). These results suggested that Notch2 and Six1 played pivotal roles in inducing EMT of lung adenocarcinoma cells.

Early-stage lung adenocarcinoma progression is assumed to be associated with an increase in the size of cancer cell nuclei (8). We measured the greatest dimension of cancer cell nuclei in 5 minimally invasive adenocarcinomas and found significantly larger nuclei in microinvasion, than in lepidic growth cancer cells from all 5 minimally invasive adenocarcinomas (Supplementary Table S1). A comparison between intact NCI-H441 cells and those transfected with the Notch2 ICD cDNA showed significantly larger nuclei in the transfectants than in the intact cells (Fig. 4B). Transfection with empty vector or with TTF-1 cDNA did not alter the size of nuclei in NCI-H441 cells (Fig. 4B).

Upregulation of Notch2 and Six1 defines a clinically aggressive phenotype of lepidic-predominant invasive adenocarcinoma

We immunohistochemically analyzed 64 samples of lepidic-predominant invasive adenocarcinoma tumors using antibodies against Notch2 and Six1. Table 1 summarizes the clinicopathologic features of each case. The immunohistochemical staining results were judged positive when more than 50% of the cancer cells in each of the lepidic growth and overt invasion components had significant cytoplasmic (Notch2) or nuclear (Six1) staining. The tumors were classified based this judgment as double (Notch2 and Six1) negative in lepidic growth, but double positive in overt invasion (N/P; $n = 23$) cells; double negative in both components (N/N; $n = 19$); double positive in both components (P/P; $n = 19$) and other ($n = 3$; summarized in Table 1). A representative staining profile of N/P tumors was shown in Supplementary Fig. S4. A statistical analysis of the clinicopathologic parameters among the groups showed that the N/P group was less favorable than the N/N group with respect to pT, pN, PL factor, and ly factor (Table 1). Univariate log-rank analyses of Kaplan–Meier survival curves revealed that DFS duration was shorter in the N/P, than in the N/N group ($P = 0.015$; Fig. 5). DFS duration was also affected by various clinicopathologic parameters including pStage, pT, pN, PL factor, and ly factor (Supplementary Table S3). Multivariate logistic regression analyses among the 3 groups revealed that the N/P and P/P groups were more likely to recur than the N/N group in 2-year postoperative follow-up (Supplementary Table S4).

Table 1. Classification of patients with lepidic-predominant invasive adenocarcinoma according to Notch2 and Six1 immunohistochemical findings

		Notch2 and Six1					
Variable	**All patients**	**N/N**	**N/P**	**P/P**	**Other**		***P***
Sex						N/N vs. N/P	0.59
Male	36	10	14	11	1	N/N vs. P/P	0.74
Female	28	9	9	8	2	N/P vs. P/P	0.85
Age						N/N vs. N/P	0.95
Mean	71	70.5	70.7	70.8	78.3	N/N vs. P/P	0.93
Range	49–86	49–86	58–83	56–85	74–85	N/P vs. P/P	0.97
pStage[a]						N/N vs. N/P	0.33
IA + IB	52	17	18	14	3	N/N vs. P/P	0.21
IIA + IIB + IIIA + IIIB	12	2	5	5	0	N/P vs. P/P	0.73
pT[a]						N/N vs. N/P	0.04
1a + 1b	39	15	11	11	2	N/N vs. P/P	0.16
2a + 2b + 3	25	4	12	8	1	N/P vs. P/P	0.52
pN[a]						N/N vs. N/P	0.03
0	55	19	18	15	3	N/N vs. P/P	0.03
1 + 2	9	0	5	4	0	N/P vs. P/P	0.96
PL factor[a]						N/N vs. N/P	0.005
0	50	18	13	17	2	N/N vs. P/P	0.55
≥1	14	1	10	2	1	N/P vs. P/P	0.02
ly Factor[a]						N/N vs. N/P	0.039
0	46	18	16	10	2	N/N vs. P/P	0.003
1	18	1	7	9	1	N/P vs. P/P	0.26
v Factor[a]						N/N vs. N/P	0.67
0	56	18	21	14	3	N/N vs. P/P	0.08
1	8	1	2	5	0	N/P vs. P/P	0.13
Tumor size (mm)						N/N vs. N/P	0.89
Mean	25.3	25.5	25	24.7	30	N/N vs. P/P	0.82
Range	11–70	11–70	15–40	12–38	15–50	N/P vs. P/P	0.87

[a]According to TNM classification (7th Edition).

Discussion

This study comprised 3 parts. A clinical issue had to be considered for the first part that compared comprehensive gene expression between lepidic growth and microinvasion cancer cells in individual minimally invasive adenocarcinomas. Because the cut surface at the greatest dimension of the tumor is used for pathologic diagnosis, remaining specimens for LMD contained only a small amount of each component, particularly the microinvasion component. The original estimated amount of total RNA used for the present DNA microarray analysis was in the order of 100 ng per component or less. This limitation might have caused considerable RNA degradation and consequently resulting in shorter aRNA probes (theoretical average length, ~1.5 kb) (Fig. 1C). Regardless, the DNA microarray analysis seemed reliable because (i) the range of the relative expression levels of 10 housekeeping genes was sufficiently small

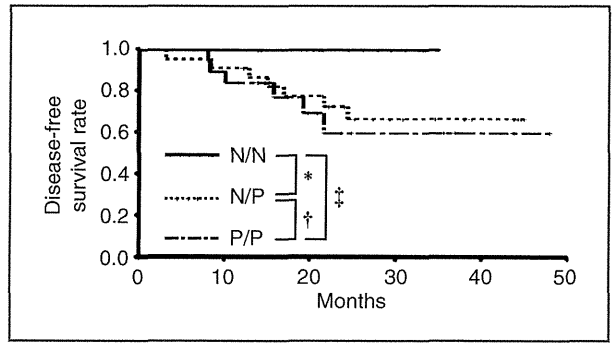

Figure 5. DFS rates of 64 lepidic-predominant invasive adenocarcinomas grouped by Notch2 and Six1 immunohistochemistry. DFS rates of N/N, N/P, and P/P tumor groups shown as function of months. The mean interval of DFS (95% CI) for N/P and P/P are 34.9 (28.8–41.1) months and 34.7 (26.2–43.2) months, respectively. Values for N/N were not calculated because N/N tumors did not recur. *, $P = 0.015$; †, $P = 0.626$; ‡, $P = 0.006$.

(within 0.5- to 2-fold) between lepidic growth and microinvasion cells (Supplementary Table S2), and (ii) differential expression of the selected 2 genes, that is, *Notch2* and *Six1* genes, was reproducibly confirmed by RT-PCR (Fig. 2A, case 1). These results indicate that tumor lesions at the early stage that contain cancer cells with different malignant potential, for example, *in situ* and invasive cells in minimally invasive adenocarcinoma, are practical for comparative gene expression analyses among cancer cells during progression *in vivo*.

Both *Notch2* and *Six1* were upregulated in microinvasion cancer cells not only in the minimally invasive adenocarcinoma that was analyzed using DNA microarrays but also in 10 other minimally invasive adenocarcinomas examined. We therefore considered that paired upregulation of Notch2 and Six1 is commonly associated with the progression of lepidic growth to microinvasion cancer cells in minimally invasive adenocarcinoma. Notch2 is a cell membrane–bound ligand-dependent receptor for the Type 1 transmembrane protein family named Notch (30–33). When Notch ligands bind to Notch2 receptors between two neighboring cells, Notch2 is cleaved through a cascade of proteolytic enzymes, including γ-secretase, and released Notch2 ICD translocates into the nucleus where it transcriptionally activates Notch2 target genes (26). Although Notch1 and Notch3, other members of the Notch family, have long been regarded as candidate molecules responsible for the development of lung cancer (34–36), whether Notch2 has similar roles remains to be determined. Six1 is a homeodomain transcription factor (37) and a putative downstream target of Notch2 (24, 25). Interestingly, Ford and colleagues showed that Six1 stimulates the malignant transformation of mammary epithelial cells through transactivating *cyclin A1* (38, 39) and induces EMT in mammary cancer cells through the induction of TGF-β signaling (27, 40). These findings suggested that Notch2 and Six1 play coordinate roles during the early-stage lung adenocarcinoma progression.

The second part of this study examined this notion using transfection experiments. Consistent with previous characterization, exogenous expression of the Notch2 ICD resulted in *Six1* transactivation in NCI-H441 lung epithelial cells. The exogenous Notch2 ICD also transactivated *Smad3*, *Smad4*, and *vimentin* in association with the downregulation of *E-cadherin*. Similar transactivation effects of Notch2 ICD were detected in 2 other types of epithelial cells derived from lung adenocarcinomas. Interestingly, Six1 was notably essential for transactivation of the 3 genes, but not for the downregulation of *E-cadherin*, suggesting that Notch2 and Six1 coordinately played a causative role in inducing EMT during the progression of lepidic growth to microinvasion cells. Exogenous expression of the Notch2 ICD in NCI-H441 cells also resulted in nuclei becoming enlarged. This was in accordance with the cytologic finding that nuclei were larger in microinvasion cancer cells than in lepidic growth cells from 5 minimally invasive adenocarcinomas examined. These results supported the notion that the transcriptional cascades activated coordinately by Notch2 and Six1 are involved in lepidic growth-to-microinvasion progression.

The third part of the study immunohistochemically investigated Notch2 and Six1 in 64 samples of lepidic-predominant invasive adenocarcinoma tumors and found that they could be assigned almost equally into groups on the basis of positive and negative staining as N/N, N/P, and P/P. Consistent with the results of the second part of the study showing that Six1 is a downstream target of Notch2, these transcription factors were either double negative or double positive in lepidic growth and overt invasion cancer cells, respectively, with some exceptions. As might be predicted from the diagnostic criteria, lepidic-predominant invasive adenocarcinoma seemed to include heterogeneous tumors with distinct natural histories and genetic alterations. Judging from the immunostaining profiles of lepidic growth and overt invasion cells, N/P tumors seem to be a simple advanced form of minimally invasive adenocarcinoma, in which microinvasion cells have grown into an overt invasion focus, and N/N tumors develop via other molecular mechanisms than those involving Notch2 and Six1. On the other hand, the origin of P/P tumors is uncertain, but they might be a more advanced form of N/P tumors. Because lepidic growth cancer cells were positive for both Notch2 and Six1, they might be potentially invasive. This speculation is reminiscent of a recent report by Anami and colleagues who notably pointed out that the lepidic growth pattern might represent the intraalveolar epithelial spread of overt invasion cancer cells (41). Whether or not lepidic growth cancer cells are invasive did not seem to affect the prognostic outcomes of patients with lepidic-predominant invasive adenocarcinomas (N/P vs. P/P in Fig. 5). Interestingly, we found that N/N tumors metastasized less often to lymph nodes, were less invasive to lymphatic vessels, and were associated with better DFS than N/P and P/P tumors ($P = 0.015$ and 0.006 by log-rank tests, respectively). These findings agree with a summary of reviews that emphasize the critical role of Notch signals in the malignant progression of non-small cell lung cancer (34–36). The paired upregulation of Notch2 and Six1 seemed to be one transcriptional alteration that is responsible for minimally invasive adenocarcinoma-to-lepidic-predominant invasive adenocarcinoma progression, and it defined a clinically aggressive phenotype subset of lepidic-predominant invasive adenocarcinoma. Because Notch2 and Six1 immunohistochemistry seemed to independently discriminate lepidic-predominant invasive adenocarcinomas with high risk of recurrence in a 2-year postoperative period, during which the recurrence of most lung cancers occurs even after curative-intent therapy (42), it could be a clinically useful examination for selecting patients with lepidic-predominant invasive adenocarcinoma needing intensive follow-up.

Aviel-Ronen and colleagues (2008) examined genomic changes associated with adenocarcinoma *in situ* and minimally invasive adenocarcinoma using array comparative

genomic hybridization and found that genomic profiles are indistinguishable between adenocarcinoma *in situ* and minimally invasive adenocarcinoma, although they developed in distinct individuals (5). In contrast, this study successfully revealed that gene expression profiles substantially differed between lepidic growth and microinvasion cancer cells in a single minimally invasive adenocarcinoma. The findings of these two studies and the present results indicate that the Notch2 and Six1 upregulation detected in minimally invasive adenocarcinoma is attributable not to particular genomic alterations, but to environmental factors, including immune and stromal cells around cancer cells. In fact, activation of the Notch2 signaling pathway is cell membrane–bound ligand dependent (26). Although further characterization of lepidic-predominant invasive adenocarcinoma is required at the molecular level, subclassification of lepidic-predominant invasive adenocarcinoma on the basis of Notch2 and Six1 upregulation seems to be clinically important in predicting the prognostic outcomes of patients with lepidic-predominant invasive adenocarcinoma.

Disclosure of Potential Conflicts of Interest

No potential conflicts of interest were disclosed.

Grant Support

This study was supported by grants from the Ministry of Education, Culture, Sports, Science and Technology of Japan and from the Nakatani Foundation of Electronic Measuring Technology Advancement.

The costs of publication of this article were defrayed in part by the payment of page charges. This article must therefore be hereby marked *advertisement* in accordance with 18 U.S.C. Section 1734 solely to indicate this fact.

Received July 28, 2011; revised December 14, 2011; accepted December 16, 2011; published OnlineFirst December 21, 2011.

References

1. Devesa SS, Bray F, Vizcaino AP, Parkin DM. International lung cancer trends by histologic type: male:female differences diminishing and adenocarcinoma rates rising. Int J Cancer 2005;117:294–9.
2. Motoi N, Szoke J, Riely GJ, Seshan VE, Kris MG, Rusch VW, et al. Lung adenocarcinoma: modification of the 2004 WHO mixed subtype to include the major histologic subtype suggests correlations between papillary and micropapillary adenocarcinoma subtypes, EGFR mutations and gene expression analysis. Am J Surg Pathol 2008;32:810–27.
3. Travis WD, Brambilla E, Noguchi M, Nicholson AG, Geisinger KR, Yatabe Y, et al. International association for the study of lung cancer/American Thoracic Society/European Respiratory Society international multidisciplinary classification of lung adenocarcinoma. J Thorac Oncol 2011;6:244–85.
4. Aoyagi Y, Yokose T, Minami Y, Ochiai A, Iijima T, Morishita Y, et al. Accumulation of losses of heterozygosity and multistep carcinogenesis in pulmonary adenocarcinoma. Cancer Res 2001;61:7950–4.
5. Aviel-Ronen S, Coe BP, Lau SK, da Cunha Santos G, Zhu CQ, Strumpf D, et al. Genomic markers for malignant progression in pulmonary adenocarcinoma with bronchioloalveolar features. Proc Natl Acad Sci U S A 2008;105:10155–60.
6. Seki N, Takasu T, Mandai K, Nakata M, Saeki H, Heike Y, et al. Expression of eukaryotic initiation factor 4E in atypical adenomatous hyperplasia and adenocarcinoma of the human peripheral lung. Clin Cancer Res 2002;8:3046–53.
7. Soh J, Toyooka S, Ichihara S, Asano H, Kobayashi N, Suehisa H, et al. Sequential molecular changes during multistage pathogenesis of small peripheral adenocarcinomas of the lung. J Thorac Oncol 2008;3:340–7.
8. Morishita Y, Fukasawa M, Takeuchi M, Inadome Y, Matsuno Y, Noguchi M. Small-sized adenocarcinoma of the lung. Cytologic characteristics and clinical behavior. Cancer 2001;93:124–31.
9. Noguchi M, Morikawa A, Kawasaki M, Matsuno Y, Yamada T, Hirohashi S, et al. Small adenocarcinoma of the lung. Histologic characteristics and prognosis. Cancer 1995;75:2844–52.
10. Maezawa N, Tsuta K, Shibuki Y, Yamazaki S, Maeshima AM, Watanabe S, et al. Cytopathologic factors can predict invasion in small-sized peripheral lung adenocarcinoma with a bronchioloalveolar carcinoma component. Cancer 2006;108:488–93.
11. Terasaki H, Niki T, Matsuno Y, Yamada T, Maeshima A, Asamura H, et al. Lung adenocarcinoma with mixed bronchioloalveolar and invasive components: clinicopathological features, subclassification by extent of invasive foci, and immunohistochemical characterization. Am J Surg Pathol 2003;27:937–51.
12. Lynch TJ, Bell DW, Sordella R, Gurubhagavatula S, Okimoto RA, Brannigan BW, et al. Activating mutations in the epidermal growth factor receptor underlying responsiveness of non-small-cell lung cancer to gefitinib. N Engl J Med 2004;350:2129–39.
13. Paez JG, Janne PA, Lee JC, Tracy S, Greulich H, Gabriel S, et al. EGFR mutations in lung cancer: correlation with clinical response to gefitinib therapy. Science 2004;304:1497–500.
14. Sakamoto H, Shimizu J, Horio Y, Ueda R, Takahashi T, Mitsudomi T, et al. Disproportionate representation of KRAS gene mutation in atypical adenomatous hyperplasia, but even distribution of EGFR gene mutation from preinvasive to invasive adenocarcinomas. J Pathol 2007;212:287–94.
15. Westra WH, Baas IO, Hruban RH, Askin FB, Wilson K, Offerhaus GJ, et al. K-ras oncogene activation in atypical alveolar hyperplasias of the human lung. Cancer Res 1996;56:2224–8.
16. Yatabe Y, Takahashi T, Mitsudomi T. Epidermal growth factor receptor gene amplification is acquired in association with tumor progression of EGFR-mutated lung cancer. Cancer Res 2008;68:2106–11.
17. Tang ZQ, Han LY, Lin HH, Cui J, Jia J, Low BC, et al. Derivation of stable microarray cancer-differentiating signatures using consensus scoring of multiple random sampling and gene-ranking consistency evaluation. Cancer Res 2007;67:9996–10003.
18. Zhang HJ, Wang HY, Zhang HT, Su JM, Zhu J, Wang HB, et al. Transforming growth factor-beta1 promotes lung adenocarcinoma invasion and metastasis by epithelial-to-mesenchymal transition. Mol Cell Biochem 2011;355:309–14.
19. Shih JY, Yang PC. The EMT regulator slug and lung carcinogenesis. Carcinogenesis 2011;32:1299–304.
20. Chiou SH, Wang ML, Chou YT, Chen CJ, Hong CF, Hsieh WJ, et al. Coexpression of Oct4 and Nanog enhances malignancy in lung adenocarcinoma by inducing cancer stem cell-like properties and epithelial-mesenchymal transdifferentiation. Cancer Res 2010;70:10433–44.
21. Li C, Cai J, Pan Q, Minoo P. Two functionally distinct forms of NKX2.1 protein are expressed in the pulmonary epithelium. Biochem Biophys Res Commun 2000;270:462–8.
22. Akagi T, Murata K, Shishido T, Hanafusa H. v-Crk activates the phosphoinositide 3-kinase/AKT pathway by utilizing focal adhesion kinase and H-Ras. Mol Cell Biol 2002;22:7015–23.
23. GEO Browser [Internet]. Bethesda (MD): National Library of Medicine (US); 2002. Expression profiling by array [cited 2011 Jul 14]. Available from: http://www.ncbi.nlm.nih.gov/geo/query/acc.cgi?token=plkbnogawiamexw&acc=GSE30663 Accession Number: GSE30663.

24. Bessarab DA, Chong SW, Korzh V. Expression of zebrafish six1 during sensory organ development and myogenesis. Dev Dyn 2004;230: 781–6.
25. Rodriguez S, Sickles HM, Deleonardis C, Alcaraz A, Gridley T, Lin DM. Notch2 is required for maintaining sustentacular cell function in the adult mouse main olfactory epithelium. Dev Biol 2008;314:40–58.
26. Fortini ME. Notch signaling: the core pathway and its posttranslational regulation. Dev Cell 2009;16:633–47.
27. Micalizzi DS, Christensen KL, Jedlicka P, Coletta RD, Baron AE, Harrell JC, et al. The Six1 homeoprotein induces human mammary carcinoma cells to undergo epithelial-mesenchymal transition and metastasis in mice through increasing TGF-beta signaling. J Clin Invest 2009; 119:2678–90.
28. Tang Y, Urs S, Boucher J, Bernaiche T, Venkatesh D, Spicer DB, et al. Notch and transforming growth factor-beta (TGFbeta) signaling pathways cooperatively regulate vascular smooth muscle cell differentiation. J Biol Chem 2010;285:17556–63.
29. Kida Y, Maeda Y, Shiraishi T, Suzuki T, Ogura T. Chick Dach1 interacts with the Smad complex and Sin3a to control AER formation and limb development along the proximodistal axis. Development 2004; 131:4179–87.
30. Grego-Bessa J, Diez J, Timmerman L, de la Pompa JL. Notch and epithelial-mesenchyme transition in development and tumor progression: another turn of the screw. Cell Cycle 2004;3:718–21.
31. Weinmaster G, Roberts VJ, Lemke G. A homolog of *Drosophila* Notch expressed during mammalian development. Development 1991; 113:199–205.
32. Jadhav AP, Mason HA, Cepko CL. Notch 1 inhibits photoreceptor production in the developing mammalian retina. Development 2006; 133:913–23.
33. Artavanis-Tsakonas S, Rand MD, Lake RJ. Notch signaling: cell fate control and signal integration in development. Science 1999;284:770–6.
34. Collins BJ, Kleeberger W, Ball DW. Notch in lung development and lung cancer. Semin Cancer Biol 2004;14:357–64.
35. Konishi J, Kawaguchi KS, Vo H, Haruki N, Gonzalez A, Carbone DP, et al. Gamma-secretase inhibitor prevents Notch3 activation and reduces proliferation in human lung cancers. Cancer Res 2007; 67:8051–7.
36. Ji X, Wang Z, Geamanu A, Sarkar FH, Gupta SV. Inhibition of cell growth and induction of apoptosis in non-small cell lung cancer cells by delta-tocotrienol is associated with Notch-1 down-regulation. J Cell Biochem 2011;112:2773–83.
37. Levine M, Hoey T. Homeobox proteins as sequence-specific transcription factors. Cell 1988;55:537–40.
38. Coletta RD, Christensen K, Reichenberger KJ, Lamb J, Micomonaco D, Huang L, et al. The Six1 homeoprotein stimulates tumorigenesis by reactivation of cyclin A1. Proc Natl Acad Sci U S A 2004;101:6478–83.
39. Coletta RD, Christensen KL, Micalizzi DS, Jedlicka P, Varella-Garcia M, Ford HL. Six1 overexpression in mammary cells induces genomic instability and is sufficient for malignant transformation. Cancer Res 2008;68:2204–13.
40. Farabaugh SM, Micalizzi DS, Jedlicka P, Zhao R, Ford HL. Eya2 is required to mediate the pro-metastatic functions of Six1 via the induction of TGF-beta signaling, epithelial-mesenchymal transition, and cancer stem cell properties. Oncogene 2011; Jun 27 [Epub ahead of print].
41. Anami Y, Iijima T, Suzuki K, Yokota J, Minami Y, Kobayashi H, et al. Bronchioloalveolar carcinoma (lepidic growth) component is a more useful prognostic factor than lymph node metastasis. J Thorac Oncol 2009;4:951–8.
42. Colice GL, Rubins J, Unger MAmerican College of Chest P. Follow-up and surveillance of the lung cancer patient following curative-intent therapy. Chest 2003;123:272S–83S.

Metabolomic analysis of dynamic response and drug resistance of gastric cancer cells to 5-fluorouracil

SHINSUKE SASADA[1], YOSHIHIRO MIYATA[1], YASUHIRO TSUTANI[1], NAOHIRO TSUYAMA[2], TSUTOMU MASUJIMA[2], JUN HIHARA[1] and MORIHITO OKADA[1]

[1]Department of Surgical Oncology, Research Institute for Radiation Biology and Medicine; [2]Analytical Molecular Medicine and Devices Laboratory, Graduate School of Biomedical and Health Sciences, Hiroshima University, Hiroshima, Japan

Received October 26, 2012; Accepted November 23, 2012

DOI: 10.3892/or.2012.2182

Abstract. Metabolomics has developed as an important new tool in cancer research. It is expected to lead to the discovery of biomarker candidates for cancer diagnosis and treatment. The current study aimed to perform a comprehensive metabolomic analysis of the intracellular dynamic responses of human gastric cancer cells to 5-fluorouracil (5-FU), referencing the mechanisms of drug action and drug resistance. Small metabolites in gastric cancer cells and 5-FU-resistant cells were measured by liquid chromatography-mass spectrometry. Candidates for drug targets were selected according to the presence or absence of resistance, before and after 5-FU treatment. In addition, the gene expression of each candidate was assessed by reverse transcription-polymerase chain reaction. The number of metabolites in cancer cells dramatically changed during short-term treatment with 5-FU. Particularly, proline was reduced to one-third of its original level and glutamate was increased by a factor of 3 after 3 h of treatment. The metabolic production of glutamate from proline proceeds by proline dehydrogenase (PRODH), producing superoxide. After 5-FU treatment, PRODH mRNA expression was upregulated 2-fold and production of superoxide was increased by a factor of 3. In 5-FU-resistant cells, proline and glutamate levels were less affected than in non-resistant cells, and PRODH mRNA expression and superoxide generation were not increased following treatment. In conclusion, the authors identified a candidate biomarker, PRODH, for drug effects using a metabolomic approach, a result that was confirmed by conventional methods. In the future, metabolomics will play an important role in the field of cancer research.

Correspondence to: Dr Morihito Okada, Department of Surgical Oncology, Research Institute for Radiation Biology and Medicine, Hiroshima University, 1-2-3 Kasumi Minami-ku, Hiroshima 734-8551, Japan
E-mail: morihito@hiroshima-u.ac.jp

Key words: metabolomics, mass spectrometry, gastric cancer, fluorouracil, amino acid, proline dehydrogenase

Introduction

Gastric cancer is common in Asia, South America and Eastern Europe, accounting for more than 800,000 new cases per year worldwide. It is also the second most common cause of cancer-related deaths globally (1). Several chemotherapy regimens have been established as the first-line therapy in the treatment of advanced gastric cancer (2-4). Nevertheless, the effectiveness of gastric cancer chemotherapy is limited, compared with similar treatment for other malignancies, such as colorectal cancer and breast cancer. Therefore, in order to improve the effectiveness of chemotherapy for this cancer, it is important to investigate the cellular responses and resistance mechanisms associated with anticancer agents.

To investigate these topics, we turned to metabolomics, which is considered the third pillar of systems biology, after genomics and proteomics, representing the end of the biochemical cascade (5). Well-recognized tools of metabolomics include gas chromatography-mass spectrometry (6), liquid chromatography-mass spectrometry (LC-MS) (7) and nuclear magnetic resonance (8). This is a novel perspective, and the comprehensive investigation of metabolic alterations in malignancies has rarely been conducted, in contrast to the well-studied genomics and proteomics fields. Moreover, only a few experiments investigating the cellular responses to chemotherapy have been reported (9-11).

Herein, we applied the LC-MS method to investigate the cellular response of gastric cancer cells to 5-fluorouracil (5-FU). We observed short-term reactions and the dynamic responses to assess the effect of the anticancer agent. In addition, we established a 5-FU-resistant cell line, MKN45/F2R, by subjecting the human gastric cancer cell line MKN45 to continuous 5-FU exposure (12). We also investigated the mechanisms of drug resistance, comparing 2 cell lines, and identified a factor, proline dehydrogenase (PRODH), that induces superoxide and is involved in the action and resistance of 5-FU. This is the first study highlighting a short-term, cellular, dynamic response of gastric cancer cells and the resistance mechanism to an anticancer agent by using the metabolomics approach.